

Understanding Large Moves in Risk-Neutral Moments

Guilherme Salomé

December 12, 2018

Abstract

We recover the 2nd, 3rd and 4th risk-neutral moments of the market index in high-frequency using the model-free measures from Fan, X. Xiao, and Zhou (2018). We analyze large moves in the risk-neutral moments, and evaluate them under the dynamics of the 3-factor Andersen, Fusari and Todorov (AFT) model. We find a big number of large moves in the risk-neutral moments, far in excess of the number of jumps in the market index. These large moves are approximately symmetric and equally divided throughout the years in the sample. We also find evidence of co-jumps between the risk-neutral variance and the market index, but less evidence for co-jumps between the market index and higher order moments. We conclude that there is evidence for the existence of a tail factor as in the AFT model.

1 Introduction

Investors' expectations of future economic conditions are what determine the current prices of assets. In a market free from arbitrage opportunities, current prices are determined by a risk-neutral measure. The risk-neutral measure is a probability distribution over future states of the world. If this measure is known, it is possible to compute the price of any asset given its possible future payoffs. In practice, however, the risk-neutral measure is unknown. Its estimation has been widely studied by the literature, where the main idea was to recover the risk-neutral distribution using observed options prices. Of particular relevance here is Bakshi and Madan (2000), which developed a model-free method of learning moments from the risk-neutral distribution. These risk-neutral moments reflect the market's expectations of future returns, and understanding their dynamics is the objective of this paper.

This paper studies the high-frequency behavior of moments of returns under the risk-neutral measure, and how these moments contrast with the implications of a recently developed options pricing model (referred to as the AFT model). In this work, I recover the 2nd, 3rd and 4th moments from the risk-neutral distribution using a model-free methodology developed in Bakshi and Madan (2000), and Fan, X. Xiao, and Zhou (2018). This methodology learns from the risk-neutral distribution using observed prices of out-of-the-money options on the S&P 500 index. Using options prices sampled every minute, the risk-neutral moments are recovered at the high-frequency, which allows for the use of high-frequency econometric tools to identify big moves in each of the moments.

The risk-neutral moments can be interpreted as the market's expectations of future returns over a specific time horizon (30 days) and are related to the expected variance, skewness and kurtosis. Therefore, big changes in these moments reflect changes in what

investors' think about future returns, and are fundamentally linked to changes in the economic environment.

The results reveal hikes in the risk-neutral moments in periods of crisis. These hikes indicate that the market's expectations regarding future variance and extreme returns increases during crises. On the other hand, in calmer periods the risk-neutral expectations about future jumps are close to zero, and the market's view of future variance is close to the actual variance.

The data also reveals that there are frequent large moves in the risk-neutral moments. Specifically, the 2nd moment jumps three times more often than the market index, while the 3rd and 4th moments jump eleven times more often than the market index. The number of jumps implies that there are revisions to market's expectations of future variance at least once every three days, and revisions to expectations of future jump returns at least once per day.

To guide the study of big moves in the risk-neutral moments, we use the Andersen, Fusari and Todorov (AFT) options pricing model. Under this model, the dynamics of the returns are driven by three factors: a short-term volatility factor, a long-term volatility factor, and a tail factor that controls the probability of a future crash. The dynamics also include jumps in the market index, which causes the volatility and the tail factor to co-jump, and jumps in the tail factor that are independent of the market index, and which only affects the probability of a future crash.

The AFT model factors are driven by economic fundamentals and can be connected to the risk-neutral moments. The connection between the risk-neutral moments and the three-factors allows for interpreting changes in market's expectations in terms of changes in the short-term volatility, long-term volatility, and the probability of a crash. This connection also implies that the dynamics of the risk-neutral moments are tied to the dynamics of the factors, and the jumps that affect them. In fact, under the dynamics of the AFT model, big changes in the second risk-neutral moment are related to price jumps, while big changes in the third and fourth moments are related to changes in the probability of a future crash.

The risk-neutral moments are studied at the high-frequency to understand whether its dynamics can be explained by the three factors from the AFT model. First, the risk-neutral moments are compared to the variables they are supposed to track: realized variance and realized jumps. This step reveals how market's expectations are aligned with real world realizations. Second, the moments are contrasted to the implications of the AFT model. Specifically, we use jumps in the market index to analyze whether the moves in the risk-neutral moments are as expected, and we use co-jump tests (see Jacod and Todorov (2009)) to verify whether there are co-moves with the market index.

We find that the implications of the AFT model only partially capture the dynamics of the risk-neutral moments recovered from the data. The model implies that the three risk-neutral moments should co-jump with the market index. We find evidence that the 2nd risk-neutral moment co-jumps with the market index, but less evidence in favor of co-jumps between the market index and the other moments. Since the 3rd and 4th moments are mostly driven by the probability of a crash, this suggests that the connection between the tail factor and the market index might differ from the estimates of Andersen, Fusari, and Todorov (2015b). Another implication of the AFT model is that there cannot be negative jumps in the 2nd risk-neutral moment. The data contradicts this implication, there are as many negative as positive jumps in the 2nd moment. The model also suggests that the tail factor (probability of crashes) can jump independently of the market index,

which is supported by the evidence of more jumps in the risk-neutral moments than in the market index.

1.1 Previous Literature

This paper is related to the literature on model-free measures of the risk-neutral distribution. Model-free measures of the risk-neutral distribution have been explored in the literature since the works of Breeden and Litzenberger (1978) and Banz and Miller (1978), which first developed a model-free measure of the risk-neutral density based on options prices. A literature review of earlier methodologies and applications is available in Christoffersen, Jacobs, and Chang (2013). The more recent literature can be divided into works that use or develop new model-free measures to compute variance, skewness and kurtosis, or tail risk. The next paragraphs outlines some of these works.

Jiang and Tian (2005) compute a model-free measure of volatility and analyze how it relates to the integrated variance under a jump-diffusion framework. Bollerslev, Tauchen, and Zhou (2009) define a variance risk premium in terms of a model-free variance. The authors use monthly data to compute the variance risk premium, and use it to explain the cross-section of returns. Bondarenko (2014) construct a model-free generalized variance, which is used to analyze the variance risk premium for the S&P 500 index. Martin (2017) defines a model-free measure of volatility named SVIX. It is related to the VIX, and it gives a lower bound on the equity premium. The author analyze its time series and concludes that there were a great increase in the equity premium during the 2008 financial crisis.

Bakshi, Kapadia, and Madan (2003) compute model-free skewness and kurtosis from options prices and decompose these measures into systematic and idiosyncratic components, which are then used to analyze the volatility smile of different assets. Neuberger (2012) build a model-free measure of skewness based on high-frequency returns, and use it to analyze how the skewness behaves at different time horizons. Conrad, Dittmar, and Ghysels (2013) follow Bakshi, Kapadia, and Madan (2003) and compute daily model-free skewness and kurtosis, and use the measures to explain stock returns. Kozhan, Neuberger, and Schneider (2013) derives a model-free measure for skewness and higher order moments. The authors use these measures to compute risk premiums and analyze how they relate to the implied volatility curve of the S&P 500.

Bollerslev and Todorov (2011) estimate a model-free tail risk measure under the risk-neutral distribution and also under the physical distribution. Their measures are based on extreme value theory. In particular, the risk-neutral tail risk measure is based on the idea that the value of OTM options close to expiration is only due to expected jumps. For example, as the time to expiration of a put option approaches zero, its value is derived only from the probability of negative jumps in the underlying asset. The authors use the tail risk estimates to construct a tail risk premium and explain market returns. Du and Kapadia (2012) construct a model-free volatility and tail risk measures using market index options. They analyze the evolution of investors' fear during financial crisis and if the measures can predict stock returns. G. Gao and Song (2013) and G. Gao, P. Gao, and Song (2018) construct a measure of disaster risk. This measure is computed using out of the money options prices, and it is defined as the difference between two other measures, which differ in the way they treat deeper OTM options. They show that their measure captures the risk-neutral expectation of a weighted sum of returns to powers greater than or equal to three, and use it to analyze returns earned by hedge funds.

Vilkov and Y. Xiao (2013) use extreme value theory to compute a model-free tail risk measure, to study the predictability of returns, and to construct portfolios that take tail risk into account. Bollerslev and Todorov (2014) and Bollerslev, Todorov, and Xu (2015) compute model-free tail risk measures following Bollerslev and Todorov (2011), but relax the assumptions on the risk-neutral jump density. Their tail risk measure is used to decompose the variance risk premium and to analyze return variation. Hao (2017) proposes a model-free tail risk index based on cumulant generating functions. Their measure is related to CBOE’s VIX and the SVIX measure of Martin (2017), and it reflects market beliefs about future crashes. The authors use changes in the index to predict market returns.

Schneider (2015) and Schneider and Trojani (2015) define model-free measures for higher order moments of the risk-neutral distribution. They use these measures to compute risk premiums for variance, skewness and kurtosis, and link them to indices of fear. R.-R. Chen, Hsieh, and Huang (2018) recover the risk-neutral density from EUR/USD options using daily data. The authors conclude that moments from the density are better predictors of future currency levels than Black-Scholes implied volatility, and that the moments can also predict some macroeconomic variables.

This paper adds to the literature of model-free measures of the risk-neutral distribution in two aspects. First, we compute the 2nd, 3rd and 4th risk-neutral moments at the high-frequency (every minute), as opposed to daily or weekly. Second, we seek to understand large moves in the risk-neutral moments and to relate them to changes in the AFT model factors.

This paper is also related to the literature that uses high-frequency options data. Cassese and Guidolin (2004) study the Italian options market using high-frequency data for options written on the MIB30 index (30 biggest italian companies). The authors analyze the information efficiency of the market. They conclude that a relevant number of options violate no-arbitrage conditions, and that the implied volatility in the options are poor predictors of future volatility in the underlying. Christensen and Nielsen (2006) study the asymptotic properties of an estimator for the co-integration relation between long memory processes. The authors apply the methodology to study the relation between the volatility implied by options and the subsequent volatility in the underlying asset, using high-frequency data to compute the volatility measures. Fahlenbrach and Sandås (2009) use high-frequency data on FTSE100 options to study its co-movements with index futures prices. The authors conclude that, in periods where the FTSE100 options are traded, moves in the options prices do not perfectly correlate with moves in the futures prices, and the authors attribute the differences to microstructure noise.

Andersen, Bondarenko, and Gonzalez-Perez (2010) and Andersen, Bondarenko, and Gonzalez-Perez (2015) use high-frequency options data to construct a model-free measure of short-term volatility, named CX. The authors study jumps in the CX measure at the minute frequency and find evidence for co-jumps with the underlying returns. They also find that these jumps are common and symmetrically distributed. Verousis and Gwilym (2011) use high-frequency options data to study return reversals and associate them to the frequency of transactions and the number of market makers. Kim and G. Lee (2011) use high-frequency options data to study changes in the risk-neutral density of the KOSPI200 index (south korean stocks) at macroeconomic news announcements. The authors conclude that the density responds to the announcements, often disappears within a day, and that the longevity and changes in skewness depend on the type of news. Birru and Figlewski (2012) uses high-frequency options data to recover the risk-

neutral density for the S&P 500 during the crisis period in 2008. The authors analyze the changes in the density before and after the crisis, and conclude that there was an increase in standard deviation, thinning of the tails and a strong pattern between the density and the market index.

Vergote and Gutiérrez (2012) use high-frequency options data to study the risk-neutral density of European interbank interest rates on days of ECB announcements. The authors conclude that the impact of the announcements on the moments of the risk-neutral distribution are persistent, and driven by surprise in interest rate changes. Kim and C. Lee (2014) study the pricing errors of different options pricing models using high-frequency data on KOSPI200 index options. The authors conclude that the best model for pricing intraday options is one with stochastic volatility and jumps, which beats a modified version of the Black-Scholes model. Audrino and Fengler (2015) use high-frequency options data to compute a realized variance for options prices. This realized variance is then compared to the options quadratic variation process under different models, and used to judge their goodness-of-fit of such models. Verousis, Gwilym, and Voukelaos (2016) uses high-frequency options data on the european market to study the effects of a reduction in the tick size on the liquidity of equity options.

The use of high-frequency options data in this paper enables the study of jumps in the risk-neutral moments. Similarly to Andersen, Bondarenko, and Gonzalez-Perez (2010) and Andersen, Bondarenko, and Gonzalez-Perez (2015), we also analyze the co-jumps between the 2nd risk-neutral moment and the underlying returns, but add to the literature in various other ways. This paper uses the test statistic from Jacod and Todorov (2009) to employ a formal co-jump test between the risk-neutral moments and the underlying. The co-jump tests are also extended to the 3rd and 4th moments, motivated by the 3-factor AFT model. Lastly, the jumps in the risk-neutral moments are interpreted under the dynamics of the AFT model.

The remaining sections of this paper are divided as follows. Section 2 discusses the computation of the model-free moments of returns under the risk-neutral distribution. These risk-neutral moments are computed at the high-frequency from options data, and are interpreted under a jump-diffusion framework. Section 3 discusses a recent options pricing model, referred to as the AFT model, in which returns are driven by three factors: short-term volatility, long-term volatility and a factor related to the probability of crashes. Section 4 discusses how this model can be used to interpret the model-free moments in terms of the three factors. Section 5 discusses preliminary results based on the analysis of jumps in the market index and in the implied moments, and contrasts the AFT model implications to what is observed in the data. Section 7 summarizes the results obtained from the analysis of the risk-neutral moments under the implications of the AFT model. Section 8.1 proposes the estimation of the AFT model using high-frequency data, and discusses the estimation strategy. Lastly, Section 8 proposes additional next steps for the continuation of this research project, and the Appendix provides details on the computation of the moments and on the high-frequency options data.

2 Model Free Measures of Moments of Return

The model free measures of moments of returns are based on no-arbitrage conditions. The absence of arbitrage allows for the use of options data to learn the moments of the risk-neutral distribution, denoted by implied moments. These implied moments can be

interpreted as market's expectations about future returns, and they allow us to understand what drives their dynamics.

This section discusses the construction and computation of the model free measures of risk-neutral moments, which were developed in the works of Carr and Madan (2001), Schneider and Trojani (2015) and Fan, X. Xiao, and Zhou (2018). The section starts with the notation used throughout the paper, and it then discusses the use of options to learn from the risk-neutral distribution. It follows by examining how to obtain moments from the risk-neutral distribution, and how to interpret those in a jump-diffusion setting. These moments, however, are affected by higher order powers of returns, and so, a method for cleaning the moments is discussed. Then, the data used in the computation of the moments is briefly discussed, and the time series of the moments is analyzed.

2.1 Notation

The price of an asset, say a stock or a market index, at time t is denoted by S_t . Its forward price for delivery at time $T > t$ is given by $F_t(T)$. If we fixed the delivery date at T , then the forward price can be simply written as F_t . The log-return for holding this futures position between times t and T is $r(t, T) \equiv \log F_T - \log F_t$. Notice the use of F_t instead of S_t in the definition of return. It allows us to avoid dealing with interest rates and dividend yields.

In order to compute the model free measures, we will make use of put and call options that are out of the money (OTM). A put option with strike price K is out of the money when $F_t > K$, and a call option with strike price K is out of the money when $F_t < K$. It is helpful to aggregate the payoffs of OTM puts and calls into a single function. Define the payoff of an OTM option with strike K and expiration T by:

$$M(K, T) \equiv \begin{cases} \max \{K - F_T, 0\}, & \text{if } F_t > K \quad (\text{payoff of OTM put}) \\ \max \{F_T - K, 0\}, & \text{if } F_t \leq K \quad (\text{payoff of OTM call}) \end{cases}$$

This function is used to obtain prices of OTM options. The price of an OTM option can be computed by taking the expectation of $M(K, T)$ under the risk-neutral distribution. The existence of a risk-neutral measure is assured under no-arbitrage conditions (see Section 6K of Duffie (2001)), and it is denoted by \mathbb{Q} . The price of an OTM option at time t is given by:

$$\Theta_t(K, T) = \mathbb{E}_t^{\mathbb{Q}}[M(K, T)]$$

Notice that the price is in terms of time- T currency, since it is not discounted by the risk-free rate. Again, this avoids dealing with interest rates and dividend yields. If $F_t > K$, then $\Theta_t(K, T)$ is the price of a put option, otherwise it is the price of a call option. The tenor of the option is written as $\tau \equiv T - t$.

2.2 Replicating Portfolios

Under the assumption of frictionless trading, Carr and Madan (2001) show that a class of smooth payoff functions can be replicated by a portfolio of out of the money options¹.

¹See Section 9.1 in the Appendix for details on the result.

Let $g : r(t, T) \mapsto g(r(t, T))$ be such a smooth payoff function, then it can be replicated by:

$$g(r(t, T)) = \int_0^\infty w(K, t, T) M(K, T) dK$$

where $w(K, t, T)$ is a weighting function that depends on the strike price K and on the form of the payoff function g . The right-hand side of this equation is the payoff of holding a portfolio of out of the money options from time t to T . This portfolio is constructed using options with different strike prices K , but with the same expiration date (T), where the portfolio weight for each option is given by $w(K, t, T)$. The payoff of this portfolio at time T is exactly the payoff defined by the function g .

Now, by taking \mathbb{Q} expectations on both sides of the equation, we obtain the cost of this portfolio at time t :

$$\mathbb{E}_t^\mathbb{Q}[g(r(t, T))] = \int_0^\infty w(K, t, T) \Theta_t(K, T) dK$$

That is, by computing the cost of the portfolio of options on the right-hand side of the equation, we learn the risk-neutral expectation of some function of the returns (left-hand side of the equation). Therefore, if we design different payoff functions g , then we can learn different aspects of the risk-neutral distribution. Notice that the replicating portfolio relies on a cross-section of out of the money options with different strike prices, but with fixed time to maturity. If we have a panel of options prices, it is possible to recover the time series of the risk-neutral expectation by computing the price of the portfolio at each time t . Since this result only relies on no-arbitrage, the time series can be computed at low or high-frequency.

We are interested in learning the second, third and fourth risk-neutral moments of returns, which can be interpreted as the market's expectations about future returns. To do so, we need to define the appropriate payoff functions and determine their replication portfolios. It is natural to consider payoffs in terms of powers of $r(t, T)$, such as $g : r \mapsto r^3$, since its replication would immediately lead to a risk-neutral moment. However, due to the restrictions on the class of g functions that can be replicated, the functions that can actually be used to recover the risk-neutral moments are slightly more involved.

Following Fan, X. Xiao, and Zhou (2018), consider a payoff function inspired by CBOE's VIX:

$$g_{\text{VIX}}(r(t, T)) \equiv 2 \left(e^{r(t, T)} - 1 - r(t, T) \right) = 2 \left(\frac{F_T - F_t}{F_t} - \ln \left(\frac{F_T}{F_t} \right) \right)$$

This payoff is twice the difference between the arithmetic return and the geometric return. From this equation alone, it is not obvious what the replication of g_{VIX} recovers from the \mathbb{Q} distribution. However, the situation is clarified by applying Taylor's theorem to g_{VIX} :

$$g_{\text{VIX}}(r) = r^2 + \frac{1}{3}r^3 + \frac{1}{12}r^4 + o(r^4)$$

That is, by replicating g_{VIX} we learn about the 2nd moment of returns, and to a lesser degree, about a linear combination of higher order moments. It is possible to show² that the cost of the replicating portfolio for g_{VIX} is given by:

$$\mathbb{E}_t^\mathbb{Q}[g_{\text{VIX}}(r(t, T))] = \int_0^\infty \frac{2}{K^2} \Theta_t(K, T) dK$$

²See Section 9.1 in the Appendix for the derivation of the replicating portfolios for all payoffs mentioned in this work.

Notice that this replicating portfolio is closely related to CBOE's VIX. In fact, the squared-VIX is a discretized version of the integral above scaled to yearly values. This equation reveals that the squared-VIX is mainly related to the variance of returns, but also to the 3rd, 4th and higher order moments of returns. Thus, by computing the price of the portfolio above we recover a combination of risk-neutral moments of returns. However, to recover the moments not in a combination, but separately, we will need two more payoff functions.

Consider the payoff function inspired by Martin (2017):

$$\begin{aligned} g_{\text{SVIX}}(r(t, T)) &\equiv (\mathrm{e}^r - 1)^2 = \left(\frac{F_T - F_t}{F_t}\right)^2 \\ &= r^2 + r^3 + \frac{7}{12}r^4 + o(r^4) \end{aligned}$$

This payoff function reveals information about the 2nd and 3rd moments of returns, and to a lesser degree, about a linear combination of higher order moments. Differently from g_{VIX} , g_{SVIX} attributes a unit weight to r^2 and r^3 , and a weight on r^4 that is different from that in g_{VIX} . This difference in weights is key to recovering the moments separately, as we discuss in the next section. It can be shown that the cost of the replication portfolio for g_{SVIX} is given by:

$$\mathbb{E}_t^{\mathbb{Q}}[g_{\text{SVIX}}(r(t, T))] = \int_0^{\infty} \frac{2}{F_t^2} \Theta_t(K, T) dK$$

Notice that it is very similar to the replicating portfolio for g_{VIX} , but with a fixed denominator in the weight function. Also, the weight function depends on the current forward price, and not on the strike price.

Lastly, consider a payoff function inspired by Kozhan, Neuberger, and Schneider (2013):

$$\begin{aligned} g_{\text{KNS}}(r(t, T)) &\equiv 6(2 + r - 2\mathrm{e}^r + r\mathrm{e}^r) \\ &= r^3 + \frac{1}{2}r^4 + o(r^4) \end{aligned}$$

Contrary to the previous two payoffs, it is not related to the 2nd moment of returns, but has loadings on the 3rd moment and, to a lesser degree, on higher order moments. It can be replicated by a portfolio with cost:

$$\mathbb{E}_t^{\mathbb{Q}}[g_{\text{KNS}}(r)] = \int_0^{\infty} 6 \frac{K - F_t}{K^2 F_t} \Theta_t(K, T) dK$$

Compared to the previous replicating portfolio cost, the weighting function now depends on both strike price and current stock price.

Each of the payoff functions above uncovers a different combination of moments of the risk-neutral distribution. However, the interpretation of these measures is made difficult by their dependence on multiple powers of r . It is possible to remove most of this dependence and obtain cleaner measures of the risk-neutral moments. The next section discusses how so.

2.3 Implied Moments

The payoff functions previously analyzed were easier to interpret when written in terms of a Taylor expansion. Notice that each of the payoffs had different coefficients for different powers of r :

$$\begin{aligned} g_{VIX}(r) &= r^2 + \frac{1}{3}r^3 + \frac{1}{12}r^4 + o(r^4) \\ g_{SVIX}(r) &= r^2 + r^3 + \frac{7}{12}r^4 + o(r^4) \\ g_{KNS}(r) &= r^3 + \frac{1}{2}r^4 + o(r^4) \end{aligned}$$

Fan, X. Xiao, and Zhou (2018) use these differences to form linear combinations of the payoffs, so that the undesired powers are eliminated:

$$\begin{aligned} g_2(r) &\equiv g_{VIX}(r) - \frac{1}{3}g_3(r) - \frac{1}{12}g_4(r) &= r^2 + o(r^4) \\ g_3(r) &\equiv g_{KNS}(r) - \frac{1}{2}g_4(r) &= r^3 + o(r^4) \\ g_4(r) &\equiv -6(g_{VIX}(r) - g_{SVIX}(r)) - 4g_{KNS}(r) &= r^4 + o(r^4) \end{aligned}$$

Observe that g_2 depends only on r^2 and on the returns to powers greater than four, but not on r^3 and r^4 , contrary to g_{VIX} , which depends on all of them. As argued by Fan, X. Xiao, and Zhou (2018), the expectation of g_2 is a cleaner measure of the 2nd moment of returns when compared to the expectation of g_{VIX} . And the expectations of g_3 and g_4 are cleaner measures of the 3rd and 4th moments of returns when compared to the expectations of g_{SVIX} and g_{KNS} . Additionally, since the conditional expectation is linear, the portfolios that replicate g_2 , g_3 and g_4 , denoted by IM2, IM3 and IM4, are determined by linear combinations of the replicating portfolios for the other payoffs:

$$\begin{aligned} \text{IM2}_t &:= \frac{1}{T-t} \mathbb{E}_t^{\mathbb{Q}}[g_2(r(t, T))] = VIX_t^2 - \frac{1}{3}\text{IM3}_t - \frac{1}{12}\text{IM4}_t \\ \text{IM3}_t &:= \frac{1}{T-t} \mathbb{E}_t^{\mathbb{Q}}[g_3(r(t, T))] = KNS_t - \frac{1}{2}\text{IM4}_t \\ \text{IM4}_t &:= \frac{1}{T-t} \mathbb{E}_t^{\mathbb{Q}}[g_4(r(t, T))] = -6(VIX_t^2 - SVIX_t^2) - 4KNS_t \\ \\ VIX_t^2 &:= \frac{1}{T-t} \mathbb{E}_t^{\mathbb{Q}}[g_{VIX}(r(t, T))] = \frac{2}{T-t} \int_0^\infty \frac{\Theta_t(K, T)}{K^2} dK \\ SVIX_t^2 &:= \frac{1}{T-t} \mathbb{E}_t^{\mathbb{Q}}[g_{SVIX}(r(t, T))] = \frac{2}{T-t} \int_0^\infty \frac{\Theta_t(K, T)}{F_t(T)^2} dK \\ KNS_t &:= \frac{1}{T-t} \mathbb{E}_t^{\mathbb{Q}}[g_{KNS}(r(t, T))] = \frac{6}{T-t} \int_0^\infty \frac{K - F_t(T)}{K^2 F_t(T)} \Theta_t(K, T) dK \end{aligned}$$

Notice that the replicating portfolios were scaled by the tenor, so that values are in units per year and comparable to well-known indices. The cost of the replicating portfolios for g_2 , g_3 and g_4 are denoted by IM (implied moments), since they recover the risk-neutral moments of returns from the options market. And, when compared to VIX^2 , $SVIX^2$ and KNS measures, the IMs are cleaner measures of the 2nd, 3rd and 4th moments of returns. Next, we interpret these cleaner measures under a jump-diffusion representation for the returns.

2.4 Interpretation of the Implied Moments

The Taylor expansion of the payoff functions shows that IM2, IM3 and IM4 recover the 2nd, 3rd and 4th risk-neutral moments of returns, up to a higher order of r . We can interpret the implied moments as market's expectations of future returns. Specifically, IM2 can be interpreted as a measure of expected variance, IM3 as a measure associated to skewness, and IM4 as a measure associated to kurtosis³. However, if we add structure to the dynamics of the returns, then we can expand the interpretation of each of the implied moments. In order to do so, consider a jump-diffusion representation for the stock price:

$$\frac{dF_t}{F_t} = \mu_t dt + \sigma_t dW_t + (e^{j_t} - 1) dN_t$$

where μ_t is the drift, σ_t the local volatility, W_t a standard Brownian motion, j_t the jump size, and N_t is a process that counts the jumps in the price and has intensity λ_t .

Under the jump-diffusion representation above, Fan, X. Xiao, and Zhou (2018) show that the implied moments are approximately:

$$\begin{aligned} \text{IM2}_t &\approx \frac{1}{T-t} \mathbb{E}_t^{\mathbb{Q}} \left[\int_t^T \sigma_s^2 ds + \int_t^T j_s^2 dN_s \right] \\ \text{IM3}_t &\approx \frac{1}{T-t} \mathbb{E}_t^{\mathbb{Q}} \left[\int_t^T j_s^3 dN_s \right] \\ \text{IM4}_t &\approx \frac{1}{T-t} \mathbb{E}_t^{\mathbb{Q}} \left[\int_t^T j_s^4 dN_s \right] \end{aligned}$$

That is, the second implied moment corresponds to the time- t expectation of the integrated variance over the period (t, T) . It depends on the diffusive variance but also on the squared jumps, and it can be interpreted as the market's expectations of future variance and jump returns. The third and fourth implied moments correspond to market's expectations of future jumps to the third and fourth powers, and do not depend on the diffusive volatility.

These results are approximations based on the dominating power of the return in the g_2, g_3 and g_4 functions, and are not exact since these functions also depend on powers of r of order greater than four. It is possible to diminish this dependency and improve the approximation by adding extra payoff functions to the linear combinations that define g_2, g_3 and g_4 . In fact, by using an increasing number of new payoff functions, it is possible to eliminate an arbitrary number of powers of r from g_2, g_3 and g_4 . The use of additional payoff functions in the computation of the implied moments is discussed in the next section.

2.5 Implied Moments with Less Higher Order Dependencies

In order to obtain even cleaner risk-neutral moments, additional payoff functions are required. To this purpose, we discuss the payoff functions proposed by Schneider and

³The skewness and kurtosis can be obtained by appropriately scaling IM3 and IM4 by IM2, and can be recovered in high-frequency from options data. This allows for an analysis of the model-free measures of variance, skewness and kurtosis following Andersen, Bollerslev, et al. (2001), which is reserved for future work.

Trojani (2015), which are defined by:

$$\begin{aligned} h_q(r) &= \frac{e^{qr} - 1 - q(e^r - 1)}{q(q-1)} \\ &= \sum_{j \geq 2} \underbrace{\frac{q^{j-1} - 1}{(q-1)j!}}_{\equiv A(j, q)} r^j \end{aligned}$$

for $q > 0$ and $q \neq 1$.

The payoff functions above depends on returns to powers 2 and greater, with coefficients given by $A(j, q)$. Schneider and Trojani (2015) show that by taking derivatives of $h_q(r)$ with respect to q , it is possible to eliminate specific powers of r . And each further derivative leads to a new payoff function:

$$g_{n-2}(r) \equiv r^n + n(n-1) \sum_{j \geq n+1} \frac{\partial^{n-2} A(j, q)}{\partial q^{n-2}} r^j \quad \text{for } n = 2, 3, \dots$$

These payoffs are called Hellinger swaps of order n . The order n determines the first power of r in the function. For example, for $n = 2$ the payoff $g_0(r)$ is a function of r to powers 2 and greater.

It is possible to show that the Hellinger swaps can be replicated, and the cost of the replicating portfolio is given by:

$$\mathbb{E}_t^{\mathbb{Q}}[g_{n-2}(r)] = n(n-1) \int_0^\infty \frac{1}{K^{3/2} F_t^{1/2}} \left[\ln \left(\frac{K}{F_t} \right) \right]^{n-2} \Theta_t(K, T) dK \quad \text{for } n = 2, 3, \dots \quad (1)$$

Now, in order to obtain implied moments that are free from the undesired powers of r , we take linear combinations of multiple Hellinger swaps (for different values of n). The dependence of the IMs on the higher order powers of r is reduced to $o(r^p)$, where p can be as big as desired, and is given by the highest order of the Hellinger swaps plus one. If the highest order used is $n = 4$, then $p = 5$ and we obtain implied moments with higher order dependencies as before. However, if the highest order used is $n = 10$, then the dependency of IM2, IM3 and IM4 on higher order powers of r is reduced to $o(r^{10})$. The only cost for using a high order n is the computation time. The algorithm for recovering the implied moments is discussed in the Appendix.

To sum up, we developed clean measures of the risk-neutral 2nd, 3rd and 4th moments under the assumption of arbitrage-free markets. These measures can be computed using only three different payoff functions but yield implied moments that depend on higher order powers of the returns. To reduce this dependency, we use additional payoff functions, Hellinger swaps. In the empirical work that follows, Hellinger swaps of order up to $n = 10$ are used to recover even cleaner measures of the 2nd, 3rd and 4th risk-neutral moments of returns, henceforth denoted as IM2, IM3 and IM4. Next, we briefly discuss the data used to compute the implied moments and then study how these model free measures behave in times of market stress.

2.6 High-Frequency Data

The implied moments are conditional expectations of returns over a given interval of time: $\mathbb{E}_t^{\mathbb{Q}}[g(r(t, T))]$. This interval is determined by the expiration date of the options

used in the replicating portfolio. For example, options which expire in 10 days lead to implied moments over the next 10 days. To produce consistent series of implied moments, it is necessary to fix a time to maturity. For historical and for comparison reasons, I fix the time to maturity to 30 calendar days. This time to maturity allows for a direct comparison to CBOE's VIX, and many other studies that use the same time frame.

The 30-days implied moments are computed using high-frequency data on the S&P 500 index options (SPX), and on the SPDR S&P 500 exchange-traded fund (SPY). The data set on the SPX options was obtained from the Chicago Board Options Exchange (CBOE). The set contains quotes at the 1-minute interval level, from 2007 to 2016, totaling 2448 days in the sample after the cleaning procedures. To provide some sense of the scale of the analysis, observe that there were 3,479,352,243 records in the raw data, and a number of techniques had to be employed in order to clean and condense the set. The data set on SPY was obtained from TickData⁴, and it contains the last closing price of every 1-minute interval, from 2007 to 2016.

There are various elements relevant to the computation of the implied moments, such as the discretization of the integrals that define the replicating portfolios, the selection of options with the correct expiration dates, the change in liquidity of options through time and bounceback filters. These elements impact the quality of the implied moments, and are discussed in detail. But due to the extension of the discussion, they are deferred to the Appendix (Section 9.2).

2.7 Time Series of the Implied Moments

The implied moments are computed in high-frequency and are plotted in Figure 1.

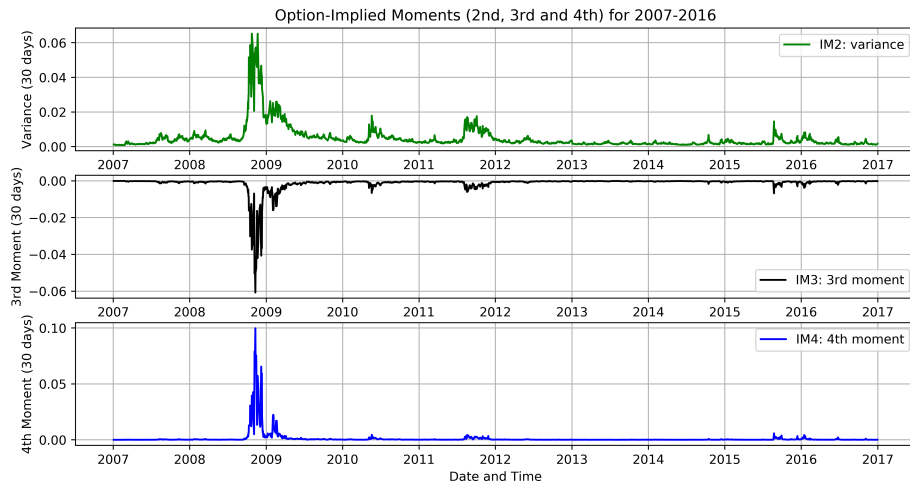


Figure 1: 2nd, 3rd and 4th implied moments computed from SPX options in high-frequency, from 2007 to 2016.

The first plot shows the risk-neutral expectation of the 2nd moment of returns (conditional variance) over the next 30 days, IM2. The units of the values are in variance per 30-days. For example, a value of 0.01 is interpreted as a conditional variance of 1%

⁴See <https://www.tickdata.com>

over the next 30 days, which corresponds to $\sqrt{0.01 \cdot \frac{365}{30}} = 34.88\%$ in units of standard deviations per year. The average value of IM2 in annualized volatility is 23.91%.

Notice that the expected volatility sharply increased during the most recent crises. Indeed, the expected volatility peaked during the 2008 financial crisis and then slowly decreased to previous levels. It then increased again in the flash crash of 2010, in the US debt ceiling crisis in 2011, and in the Chinese stock market turbulence in 2015-2016.

The second plot shows the expected 3rd moment of returns over the next 30 days, $IM3$. The third moment is related to the skewness of returns. A negative value means market's expect that returns are more prone to crash, than to hike. Notice that the values are always negative, and become more negative during moments of turmoil. In particular, IM3 became very negative during the 2008 crisis, implying that market's expected very negative returns in the near future. IM3 also reverts to the mean faster than IM2. For example, in the 2008 financial crisis IM2 returned to pre-crisis values only at the end of 2009, while IM3 had returned to pre-crisis values within the first quarter of 2009. In calmer periods, the value of IM3 gets closer to zero, indicating a lowering in market's expectations about future crashes.

The last plot displays the expected 4th moment of returns over the next 30 days, $IM4$. The fourth moment is related to the kurtosis of returns. An increase in $IM4$ means market's expect the returns to have fatter tails (higher possibility of extreme returns). IM4 is always positive and increases during periods of crisis. It also reverts to the mean faster than both IM3 and IM2. Like IM3, IM4 gets closer to zero in calmer periods, indicating a lowering in market's expectations about future extreme returns.

Overall, the plots show that all implied moments react to crises, and IM3 and IM4 have a faster return to the mean than IM2. The plots also indicate that after periods of crises are over, market's view about the 3rd and 4th moments quickly approach zero.

So far, we interpreted the implied moments only under no-arbitrage. If we consider the market jump-diffusion process approximation discussed previously, then it is possible to interpret the implied moments in terms of variance and jump returns.

2.8 Implied Moments and Forward Realized Moments

Under the jump-diffusion setting discussed previously, the implied moments approximate expectations of future variance and jump returns under the risk-neutral measure. Therefore, it is natural to compare the risk-neutral implied moments (expectations) to their future realizations under the physical measure. Figure 2 plots IM2 and the forward realized variance computed from high-frequency S&P500 prices.

The first plot displays the forward realized variance in red, and IM2 in green. $IM2_t$ is a forward looking measure and uses information up to time t to compute the expected variance (under \mathbb{Q}) over the next 30 days. The forward realized variance (FRV_t) measures the actual variance over the same period and is computed using information up to time $t + 30$ days. This difference in time implies $IM2_t$ is naturally a lagging indicator of FRV_t . Observe that whenever there is a hike in FRV, IM2 soon follows, but overshoots the increase in the variance. This effect is evident in the 2008 crisis, but also happens in all other crises in 2007-2016. Even after the variance decreases, the expectation of the variance remains high, and takes a long time to decrease to the previous level, always remaining above the actual variance. The second plot displays the difference between FRV and IM2. The curve is almost always below zero, and becomes positive after a hike in RV, but then sharply decreases as investors update their expectations. The figure

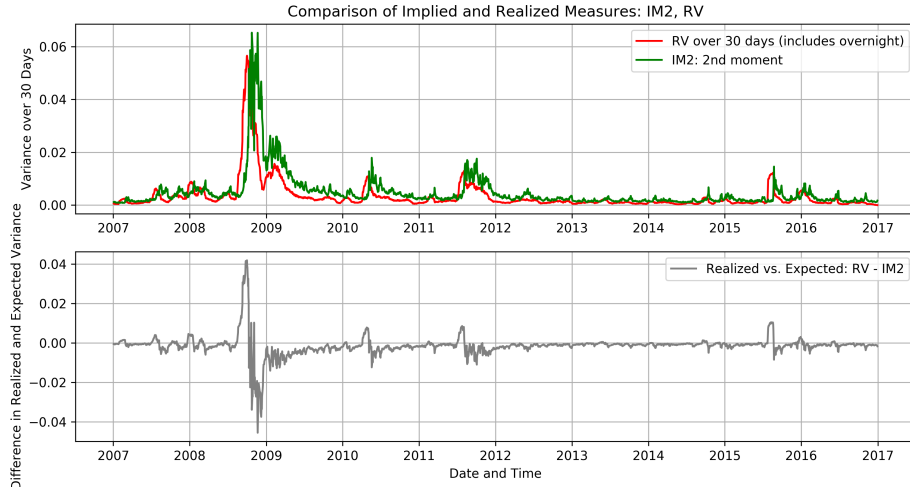


Figure 2: 2nd implied moment (green line) and forward realized variance (red line) from 2007 to 2016. Forward realized variance computed from 1-minute S&P500 prices.

suggests that after the initial turmoils of a crisis, the risk-neutral expected variance is consistently higher than the realized variance, which reflects the volatility risk premium results from Bollerslev, Tauchen, and Zhou (2009).

Next, we compare IM3 to the realized jumps. Figure 3 displays the results.

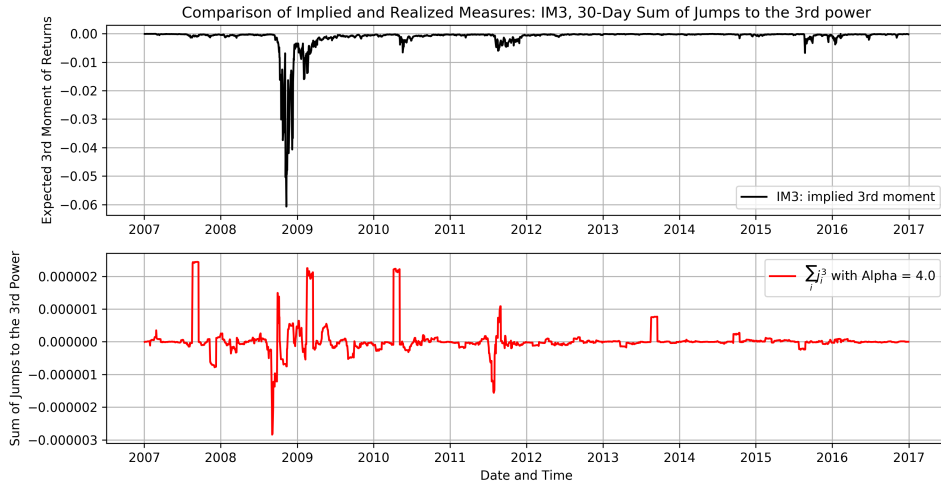


Figure 3: 3rd implied moment (black line) and sum of jumps to the 3rd power (red line) from 2007 to 2016. The jump returns were obtained using a threshold of $\alpha = 4$.

IM3 measures market's risk-neutral expectation of jumps in the near future. Specifically, it is an approximation of the risk-neutral expectation of the sum of jump returns to the 3rd power over the next 30 days. It can be compared to the actual sum of jump returns to the 3rd power over the same period. We refer to this sum as the realized jumps henceforth. Contrary to the expected and realized variance plots, IM3 does not seem to track the realized jumps. IM3 suggests that market's view negative jump returns as more likely than positive jump returns, and more intensely so in periods of crisis. The realized jumps, however, indicate that both negative and positive jump returns occur in the short

term. In fact, if negative jump returns were more likely under the physical measure, then the red curve should be mostly negative. Even in the 2008 crisis the realized jumps shift between negative and positive values, indicating that jumps of opposite sign occurred within the 30 days periods.

Figure 4 compares IM4 to the realized jumps. In this case, the realized jumps are the sum of the realized jump returns to the 4th power.

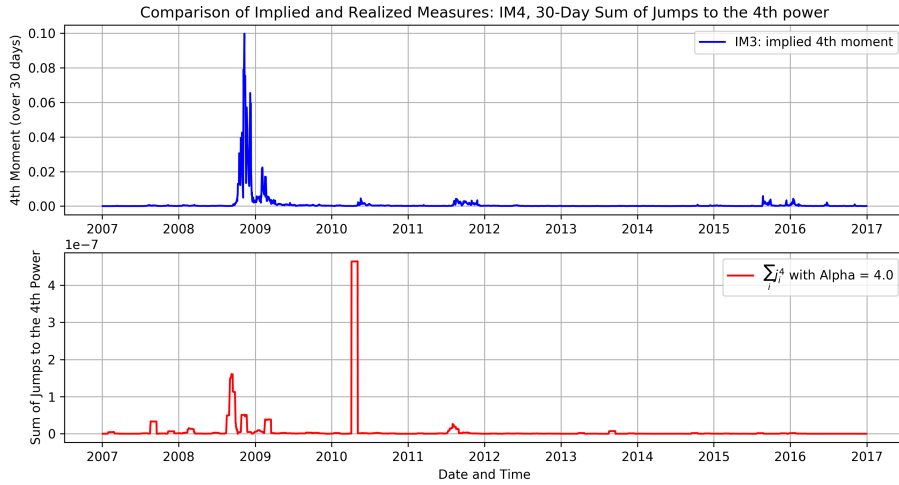


Figure 4: 4th implied moment (blue line) and sum of jumps to the 4th power (red line) from 2007 to 2016. The jump returns were obtained using a threshold of $\alpha = 4$.

The plots show that IM4 is a lagging indicator of the realized jumps during periods of crisis. The plots also reveal that extreme jump returns were expected during the 2008 crisis. To see how extreme, consider the value of 0.04 for IM4 at the end of 2008. If we expected a single jump in the next 30 days, that 0.04 translates to a jump return of $0.04^{\frac{1}{4}} = 44.7\%$. However, there is a significant difference between the scale of IM4 and that of the realized jumps. Even in the 2008 crisis, the realized jumps did not sum up to such high numbers, which means that market's consider jump returns to have very fat tails under the risk-neutral distribution. If we consider the peak value of the actual sum of jump returns in 2008, and, for simplicity, that it was due to a single jump, the value of about $1.8 \cdot 10^{-7}$ translates to a jump return of $(1.8 \cdot 10^{-7})^{\frac{1}{4}} = 2.05\%$. This wedge between the risk-neutral expectation and realized jump returns diminished after the 2008 crisis, as reflected by much smaller peaks in IM4 on the subsequent crises.

In summary, the contrast between the risk-neutral moments and the realizations under the physical distribution reveal the differences in market's views regarding future variance and jump returns. Specifically, under the risk-neutral distribution, market's expect a higher variance than is realized, and the expected variance is almost always above the realized. Additionally, in periods of crisis market's expect more crashes than actually happen, and assign a higher probability to extreme returns. In calmer periods, the market's expectation of future variance is close to the actual variance, and expectations about future jump returns are close to zero.

3 The 3-Factor AFT Model

The implied moments are model free measures, since their existence only relies on the assumption of no-arbitrage. Under no-arbitrage, IM2, IM3 and IM4 can be interpreted as measures related to risk-neutral variance, skewness and kurtosis of the index returns. Since the implied moments are risk-neutral expectations, it is also natural to interpret them as the market's expectations of future returns. Under the assumption that the returns follow a jump-diffusion process, the implied moments can be interpreted in a new way. IM2 can be interpreted as the market's expectation of future diffusive variance and squared jump returns. And IM3 and IM4 can be interpreted as market's expectations of the sum of future jump returns to the third and fourth powers.

In this section, we employ additional structure to guide the interpretation of large moves in the risk-neutral moments. This structure is given by an options pricing model recently developed in Andersen, Fusari, and Todorov (2015a) and Andersen, Fusari, and Todorov (2015b), and henceforth referred to as the AFT model (or the AFT 3-factor model). This model adds to the interpretation of the implied moments by connecting them to three factors: a short-term volatility factor, a long-term volatility factor and a factor that drives the probability of crashes (tail risk factor). The gains from this are twofold. First, the three factors can be quantified. It is possible to recover the values of the volatility and tail risk factors from the estimation of the AFT model. In fact, the estimation of the model with high-frequency data recovers the factors in high-frequency, which can then be used to study big moves in the implied moments. Second, changes in the implied moments can be interpreted in terms of the factors. Using the tools of high-frequency econometrics, we can identify big moves in the implied moments and study them in terms of changes in the AFT factors.

This section goes through the development of the AFT model in a series of steps. It starts by explaining the features of a more basic model, the 2-factor Heston model, and then builds upon it until the 3-factor AFT model is obtained. If the reader is familiar with equations 2 and 3, skip to Section 3.5.

3.1 Starting Point: 2-factor Heston model

Consider a 2-factor Heston model based on Christoffersen, Heston, and Jacobs (2009):

$$\begin{aligned}\frac{dX_t}{X_{t-}} &= \overbrace{(r_t - \delta_t)dt}^{\text{drift}} + \sqrt{V_{1,t}}dW_{1,t}^{\mathbb{Q}} + \sqrt{V_{2,t}}dW_{2,t}^{\mathbb{Q}} \\ dV_{1,t} &= \kappa_1(\bar{v}_1 - V_{1,t})dt + \sigma_1\sqrt{V_{1,t}}dB_{1,t}^{\mathbb{Q}} \\ dV_{2,t} &= \kappa_2(\bar{v}_2 - V_{2,t})dt + \sigma_2\sqrt{V_{2,t}}dB_{2,t}^{\mathbb{Q}}\end{aligned}$$

These equations define the risk-neutral dynamics for the market index X_t and for the volatility factors $V_{1,t}$ and $V_{2,t}$.

The index returns follow a diffusion process, and depends on a drift and two volatility factors ($V_{1,t}$ and $V_{2,t}$). The drift controls the average stock return. It is given by the difference between the interest rate r_t and the dividend yield δ_t . Intuitively, the drift is how much an investor expects a stock to appreciate in a risk-neutral world. The volatility factors determine the stochastic deviations of the return from its mean. These deviations are given by Gaussian shocks, modeled by two uncorrelated standard Brownian motions $W_{1,t}^{\mathbb{Q}}$ and $W_{2,t}^{\mathbb{Q}}$, multiplied by the square-root of the volatility factors.

The volatility factors themselves are also diffusions. Each factor V_i gravitates towards a long-run value, given by \bar{v}_i . The speed at which V_i approaches its long-run value is dictated by the mean reversal parameter κ_i . Higher values of κ_i mean V_i reverts faster to its long-run value. V_i is also affected by random Gaussian shocks, modeled by a standard Brownian motion $B_{i,t}^{\mathbb{Q}}$. The volatility of the changes in V_i (volatility of the volatility) is determined by σ_i . It is assumed that the shocks to each volatility factor are independent: $\text{Corr}(B_{1,t}^{\mathbb{Q}}, B_{2,t}^{\mathbb{Q}}) = 0$. But they might be correlated with price shocks: $\text{Corr}(W_{1,t}^{\mathbb{Q}}, B_{1,t}^{\mathbb{Q}}) = \rho_1$, $\text{Corr}(W_{2,t}^{\mathbb{Q}}, B_{2,t}^{\mathbb{Q}}) = \rho_2$.

As argued by Bates (2000), and many others in the literature, the volatility factor $V_{1,t}$ was first introduced to capture the volatility smirk present in options prices. The introduction of $V_{1,t}$ allows return and volatility to be negatively correlated⁵. This increases the probability of negative returns within the model, so that the distribution of the prices becomes negatively skewed. The negative skewness makes out-of-the-money options more valuable, capturing the volatility smirk. In terms of parameters, the skewness of the price distribution is controlled by ρ_1 , and the kurtosis is controlled by σ_1 .

Christoffersen, Heston, and Jacobs (2009) introduced the second volatility factor, $V_{2,t}$. In their work, the authors substantiate that the level of the volatility smirk moves independently of its slope. That is, the degree to which out-of-the-money options are priced above the Black-Scholes prices (determined by the skewness) is not dependent on the current level of volatility. The authors argue that a model with only one volatility factor imposes a tight restriction between skewness and the current volatility level. This restriction motivates the inclusion of the second volatility factor.

The different dynamics of skewness and volatility level are captured by the difference in the mean reversal speed of the two volatility factors. $V_{1,t}$ has high mean reversal, capturing short-term variance, while $V_{2,t}$ has low mean reversal, modeling long-term variance. As a consequence, the model's correlation between return and variance becomes stochastic. The stochastic correlation allows the model to capture the time variation of skewness without hinging on the level of the volatility.

3.2 2-factor Heston model with price jumps

While the 2-factor Heston model works well in comparison to earlier models, it has difficulty in pricing short-term out-of-the-money options. According to Bakshi, Cao, and Z. Chen (1997), this is due to the volatility factors following a diffusion process. The diffusion assumption means the volatility factors have continuous sample paths, restricting how fast they can change. Thus, the factors are unable to incorporate abrupt changes in the options skewness and kurtosis, and fail to price short-term OTM options. Bates (2000) also argues that the 2-factor model requires extreme parameter values to generate the observed (implied) levels of negative skewness.

Since the main issue with the 2-factor Heston model is capturing quick changes in

⁵The empirically observed negative correlation between return and volatility is usually referred to as the leverage effect or the volatility feedback effect. These terms refer to two complementary explanations for the observed correlation. The leverage effect explanation is that negative stock returns lead to the reduction of a firm's value, which is associated with increased financial risk, increasing its price volatility. The volatility feedback explanation is that higher volatility leads to an increased discount rate, and thus a reduction in the stock price. See Black (1976) (reprinted in Andersen and Bollerslev (2018)) for the leverage effect, and Poterba and Summers (1986) and Campbell and Hentschel (1992) for the volatility feedback.

skewness, it is natural to consider an extension that allows for discontinuous distributional changes. These discontinuous changes are accomplished by allowing returns to jump:

$$\begin{aligned}\frac{dX_t}{X_{t-}} &= (r_t - \delta_t)dt + \sqrt{V_{1,t}}dW_{1,t}^{\mathbb{Q}} + \sqrt{V_{2,t}}dW_{2,t}^{\mathbb{Q}} + \int_{\mathbb{R}} (\mathrm{e}^x - 1)\tilde{\mu}^{\mathbb{Q}}(dt, dx) \\ dV_{1,t} &= \kappa_1(\bar{v}_1 - V_{1,t})dt + \sigma_1\sqrt{V_{1,t}}dB_{1,t}^{\mathbb{Q}} \\ dV_{2,t} &= \kappa_2(\bar{v}_2 - V_{2,t})dt + \sigma_2\sqrt{V_{2,t}}dB_{2,t}^{\mathbb{Q}}\end{aligned}$$

The term in dark green modifies the dynamics of the index returns by allowing them to change more abruptly than what was possible with the diffusive volatility factors. This term is referred to as the jump process. The jump process is a stochastic process that models the arrival of discrete moves (jumps) at random times. It depends on a jump measure $\tilde{\mu}^{\mathbb{Q}}$ and on a distribution for the jump sizes.

The jump measure $\tilde{\mu}^{\mathbb{Q}}(dt, dx)$ determines the arrival of unexpected jumps, and itself depends on a counting process $\mu(dt, dx)$ and on its jump intensity. The counting process $\mu(dt, dx)$ is a process that puts probability mass whenever there is a jump. Intuitively, it is like a switch that turns on if there is a big move in the stock price, but is turned off otherwise. The jump intensity of the counting process is given by $dt \otimes v_t^{\mathbb{Q}}(dx)$, and measures the expected number of jumps of size x at a time interval. These two terms define the jump measure $\tilde{\mu}^{\mathbb{Q}}(dt, dx) \equiv \mu(dt, dx) - dtv_t^{\mathbb{Q}}(dx)$.

The jump process also depends on the distribution of the jump sizes. In this case, the jumps are modeled by an exponential distribution. Kou (2002) argues for exponentially distributed price jumps based on empirical evidence from behavioral finance. Kou's argument is that markets overreact and underreact to good and bad news, and that price jumps can be interpreted as the market's reaction to outside news. The exponential distribution, which has heavy tails and a high peak, serves to model overreaction (heavy tails) and underreaction (high peak) to news.

The exponential distribution considered here is an asymmetric double exponential distribution. It allows negative and positive jumps to have different tail decays. The conditional distribution of these jumps is characterized by the jump compensator, which is given by:

$$\frac{v_t^{\mathbb{Q}}(dx)}{dx} = c^-(t)1_{\{x<0\}}\lambda_-e^{-\lambda_-|x|} + c^+(t)1_{\{x>0\}}\lambda_+e^{-\lambda_+|x|}$$

The compensator implies that negative jumps are exponentially distributed with parameter λ_- , while positive jumps are exponentially distributed with parameter λ_+ . The parameters λ_- and λ_+ dictate how fast the exponential distribution decays: smaller values imply heavier tails. The intensities of the negative and positive jumps are given by $c^-(t)$ and $c^+(t)$, defined below:

$$\begin{aligned}c^-(t) &= c_0^- + c_1^-V_{1,t-} + c_2^-V_{2,t-} \\ c^+(t) &= c_0^+ + c_1^+V_{1,t-} + c_2^+V_{2,t-}\end{aligned}$$

The intensities determine the probabilities of negative and positive jumps. They are time-varying and change with the volatility factors. Bates (2000) argues that it is implausible to have constant jump intensities due to big changes observed in the implied volatility, which motivates the inclusion of the volatility factors in c^- and c^+ .

The inclusion of jumps provides another channel for modifying the returns distribution. Specifically, the skewness is controlled by the correlation of the return and the

volatility factors but also by the average jump size. The kurtosis is controlled by the volatility of the volatility and also by the volatility of the jump size. Because the jumps are not restricted to continuous moves, this model can capture sudden changes in the price skewness. Bates (2000) estimates a 2-factor model with jumps in stock returns, and concludes that jumps indeed improve the pricing of short-term OTM options, and generate more plausible volatility values.

3.3 2-factor Heston model with price and volatility jumps

Eraker, Johannes, and Polson (2003) argue that the conditional volatility of returns can move too fast to be compatible with the 2-factor model with price jumps. This is due to two main issues. The first is that, although price jumps can generate large moves, their impacts are short-lived, and have no effect on the future distribution of returns. The second is that the volatilities have continuous paths, so sudden large moves cannot be modeled. For example, the model cannot incorporate jumps in the stock price, that are subsequently followed by bigger returns due to an increased volatility level. This is because the jump itself does not change the future distribution of returns, and while the volatility factors does change the future distribution of returns, it cannot change fast enough to accommodate the subsequent big returns.

To bridge the gap between jump returns and increased (or decreased) volatility levels, Eraker, Johannes, and Polson (2003) introduce volatility jumps. Consider the 2-factor Heston model extended for jumps in prices and in the first volatility factor:

$$\begin{aligned} \frac{dX_t}{X_{t-}} &= (r_t - \delta_t)dt + \sqrt{V_{1,t}}dW_{1,t}^{\mathbb{Q}} + \sqrt{V_{2,t}}dW_{2,t}^{\mathbb{Q}} + \int_{\mathbb{R}} (e^x - 1)\tilde{\mu}^{\mathbb{Q}}(dt, dx) \\ dV_{1,t} &= \kappa_1(\bar{v}_1 - V_{1,t})dt + \sigma_1 \sqrt{V_{1,t}}dB_{1,t}^{\mathbb{Q}} + \mu_1^- \int_{\mathbb{R}} x^2 1_{\{x<0\}} \mu(dx) + \mu_1^+ \int_{\mathbb{R}} x^2 1_{\{x>0\}} \mu(dx) \\ dV_{2,t} &= \kappa_2(\bar{v}_2 - V_{2,t})dt + \sigma_2 \sqrt{V_{2,t}}dB_{2,t}^{\mathbb{Q}} \end{aligned}$$

The specification allows for co-jumps in the stock price and in the volatility, and captures the dynamics that the previous models failed to. The jumps in the volatility factor $V_{1,t}$ are connected to the jumps in the stock price in a deterministic way. The deterministic link is justified by Andersen, Fusari, and Todorov (2015b). They claim there is empirical evidence for GARCH-type dynamics in the volatility, and that the specification above is the continuous-time analog.

Observe that the volatility jumps are given by the square of exponentially distributed random variables. According to Andersen, Fusari, and Todorov (2015b), this makes the jumps have heavier tails, and intensifies the reaction of the volatility to large price jumps. Also note that negative price jumps and positive price jumps impact the volatility differently. This different impact is due to the leverage effect, negative returns correlate with increases in volatility ($\mu_1^- > 0$), while positive returns correlate with reductions in volatility ($\mu_1^+ < 0$).

Eraker, Johannes, and Polson (2003) estimate a similar model, and compare it to the previous models in the literature that did not consider volatility jumps. The authors conclude that models without volatility jumps are misspecified, and the addition of volatility jumps increases the implied volatility for OTM options, better capturing the volatility smirk.

3.4 The 3-factor AFT model

Andersen, Fusari, and Todorov (2015a) notice that a 1-factor model with price and volatility jumps produces persistent biases in pricing options in the aftermath of crises. Specifically, from 1997 to 1999 and from 2008 to 2010, the model persistently under prices short-maturity OTM options, and persistently overprices short-maturity ATM options. They argue that the cause of misspricing is the link between the risk factors in the model: volatility and jumps. They explain that the prices of short-term OTM options are mainly determined by the left tail of the jump risk, while the price of short-term ATM options are mostly determined by the current level of diffusive volatility. The tension between the pricing of short-maturity OTM options and ATM options is due to the direct link between the distribution of jumps and the diffusive volatility. As an example, notice that in the 2-factor Heston model with price and volatility jumps, the jump intensity, which characterizes the distribution of jumps, is given by a linear combination of the volatility factors. In this model, changes in the volatility factors led to changes in the jump intensity, and caused the difficulties in pricing short-term OTM options and short-term ATM options.

Andersen, Fusari, and Todorov (2015a) propose loosening the link between jumps and volatility by introducing a new factor that influences the jump distribution but does not depend on the diffusive volatility. Specifically, they introduce a tail factor that drives the jump intensity, and is driven by price co-jumps and by jumps independent of volatility jumps. The model takes the specification below:

$$\begin{aligned} \frac{dX_t}{X_{t-}} &= (r_t - \delta_t)dt + \sqrt{V_{1,t}}dW_{1,t}^{\mathbb{Q}} + \sqrt{V_{2,t}}dW_{2,t}^{\mathbb{Q}} + \int_{\mathbb{R}^2} (e^x - 1)\tilde{\mu}^{\mathbb{Q}}(dt, dx, dy) \\ dV_{1,t} &= \kappa_1(\bar{v}_1 - V_{1,t})dt + \sigma_1\sqrt{V_{1,t}}dB_{1,t}^{\mathbb{Q}} + \mu_1 \int_{\mathbb{R}^2} x^2 1_{\{x<0\}}\mu(dt, dx, dy) \\ dV_{2,t} &= \kappa_2(\bar{v}_2 - V_{2,t})dt + \sigma_2\sqrt{V_{2,t}}dB_{2,t}^{\mathbb{Q}} \\ dU_t &= -\kappa_u U_t dt + \mu_u \int_{\mathbb{R}^2} [(1 - \rho_u)x^2 1_{\{x<0\}} + \rho_u y^2] \mu(dt, dx, dy) \end{aligned} \quad (2)$$

The risk-neutral dynamics for the tail factor U_t are given in the last line of the equation. But before exploring the dynamics of U_t , notice two main differences from the 2-factor Heston model with price and volatility jumps. The first is that positive price jumps no longer affect $V_{1,t}$. As argued by Andersen, Fusari, and Todorov (2015b), this is for parsimony and ease of identification when estimating the model from options data. The second, is that the jump measure now has a dy term, which is due to the dynamics of U_t , and is given by $\tilde{\mu}^{\mathbb{Q}} \equiv \mu(dt, dx, dy) - dtv_t^{\mathbb{Q}}(dx, dy)$.

The tail factor follows a drift and a jump process. The drift has a mean reversion parameter κ_u and a long-run value of zero. The jump process is affected by two types of jumps: price co-jumps (referred to as x jumps), and jumps independent to the volatility (referred to as y jumps). Price co-jumps in U_t are proportional to the jumps in $V_{1,t}$, with the parameter ρ_u controlling the proportionality. If $\rho_u = 0$, U_t has no independent jumps, and is driven exclusively by price co-jumps. If $\rho_u = 1$, then U_t is driven exclusively by independent jumps (y jumps). The other type of jumps that affect U_t are independent jumps. Similarly to the volatility factor jumps, the y jumps are exponentially distributed and enter the U_t dynamics squared. Also notice that, like $V_{1,t}$, U_t is only affected by negative price jumps (due to identification issues).

The U_t factor affects the model dynamics via the jump intensity, and it does so separately of $V_{1,t}$. The connection of U_t with negative jumps allows the model to capture

an increase in the intensity of jumps during periods of crisis. The introduction of the tail factor changes the jump compensator and the jump intensities, which are now given by:

$$\frac{v_t^{\mathbb{Q}}(dx, dy)}{dxdy} = \begin{cases} c^-(t)1_{\{x<0\}}\lambda_-e^{-\lambda_-|x|} + c^+(t)1_{\{x>0\}}\lambda_+e^{-\lambda_+|x|}, & \text{if } y = 0, \\ c^-(t)\lambda_-e^{-\lambda_-|y|}, & \text{if } x = 0 \text{ and } y < 0 \end{cases} \quad (3)$$

$$c^-(t) = c_0^- + c_1^-V_{1,t-} + c_2^-V_{2,t-} + c_u^-U_{t-}$$

$$c^+(t) = c_0^+ + c_1^+V_{1,t-} + c_2^+V_{2,t-} + c_u^+U_{t-}$$

The compensator is split in two cases. The first is when there is a price jump, and the second is when there is an independent jump in U_t . For price jumps we still have the same asymmetric double exponential distribution, but with a change in the jump intensities: they now depend on U_t . Independent jumps also follow an exponential distribution, and use the same tail decay and jump intensity as the negative price jumps. Notice that the jumps in U_t are strictly positive.

The jump intensities depend on both volatility factors, but also on the tail factor. This allows the intensity of the jumps to move separately from the diffusive volatility, alleviating the tension between pricing short-maturity OTM and ATM options. The model also allows cross-excitation, where jumps in volatility lead to an increased probability that U_t will increase in the future, and vice-versa. Lastly, the model allows for differences between the arrival of negative and positive jumps.

3.5 Interpreting the 3-factor AFT model

Before using the AFT model to interpret the risk-neutral moments, we first discuss the interpretation of the model factors (volatilities and tail factor) in the context of the parameters estimates from Andersen, Fusari, and Todorov (2015b). The parameters estimates and their interpretations are summarized in Table 1.

The volatility factors follow similar processes, but present different dynamics: short-term variations are modeled by $V_{1,t}$, and long-term variations by $V_{2,t}$. The parameters estimates confirm these different dynamics. Indeed, notice that $V_{1,t}$ reverts to the mean faster than $V_{2,t}$, implying that changes in $V_{1,t}$ are less persistent than changes in $V_{2,t}$. This is exemplified by the half-life of these factors: Andersen, Fusari, and Todorov (2015b) argue that the half-life of $V_{1,t}$ is of three weeks, while that of $V_{2,t}$ is of five months. Notice also that $V_{1,t}$ is more volatile and has a lower long-run value than $V_{2,t}$. The higher variability of $V_{1,t}$ means it drives the index volatility in the short-term. And the higher long-run value of $V_{2,t}$, means it drives the volatility in the long-run. Thus, $V_{1,t}$ captures short-term volatility dynamics, and $V_{2,t}$ captures the long-term (persistent) dynamics. Both factors are also negatively correlated with the returns, which is expected due to the leverage effect, and determine the spot volatility of the model. The spot volatility is given by $\sqrt{V_{1,t} + V_{2,t}}$, and sums up to 11.4% per year using the long-run values for the volatility factors.

The tail factor also has a mean reversal parameter, and can be compared to the volatility factors in terms of persistence. The mean reversal estimate for the tail factor implies it is even more persistent than $V_{2,t}$. In fact, while the half-life of $V_{2,t}$ is five months, the half-life of U_t is eight years. This means U_t decays very slowly and can impact the pricing of OTM options with both short and long maturities.

The factors are all related to the probability of jumps in the AFT model. However, the parameter estimates reveal that the negative jump intensity is affected only by $V_{1,t}$

	Parameters	AFT Estimates	Interpretation
Factors	$V_{1,t}$	κ_1	10.989 Mean reversion speed
		\bar{v}_1	0.003 Long-run factor value
		σ_1	0.249 Volatility of volatility
		μ_1	12.158 Multiplier for negative price jumps
		ρ_1	-0.959 Correlation between $W_{1,t}^Q, B_{1,t}^Q$
	$V_{2,t}$	κ_2	1.864 Mean reversion speed
		\bar{v}_2	0.01 Long-run factor value
		σ_2	0.17 Volatility of volatility
		ρ_2	-0.979 Correlation between $W_{2,t}^Q, B_{2,t}^Q$
	U_t	κ_u	0.0877 Mean reversion speed
		μ_u	7.124 Multiplier for jumps
		ρ_u	0.5 Contribution of independent jumps to the tail factor
Compensator	v_t^Q	λ_-	25.944 Tail decay for negative jumps
		λ_+	36.62 Tail decay for positive jumps
	$c^-(t)$	c_0^-	0.0 Constant intensity for negative jumps
		c_1^-	111.061 Intensity contributed by $V_{1,t}$
		c_2^-	0.0 Intensity contributed by $V_{2,t}$
		c_u^-	1.0 Intensity contributed by U_t
	$c^+(t)$	c_0^+	0.372 Constant intensity for positive jumps
		c_1^+	25.855 Intensity contributed by $V_{1,t}$
		c_2^+	81.719 Intensity contributed by $V_{2,t}$
		c_u^+	0.0 Intensity contributed by U_t

Table 1: Summary of the 3-factor AFT model parameters, with interpretations and estimated values (from Andersen, Fusari, and Todorov (2015b)). The authors estimated the model using data on S&P 500 equity-index options (SPX). Their data covered the period of 1993 to 2013, with options prices sampled at Wednesdays (daily average of 234 bid-ask quotes).

and U_t , while the positive jump intensity is affected only by $V_{1,t}$ and $V_{2,t}$. That is, the short term volatility drives both the probability of negative and positive jumps, but the long-term volatility only drives the probability of positive jumps, and the tail factor only drives the probability of negative jumps. Nevertheless, notice that the contributions of all factors to the jump intensities are positive: an increase in one of the factors increases the corresponding jump intensity. Also notice that the short-term volatility has a bigger impact on c^- than on c^+ , so that increases in the $V_{1,t}$ leads to a higher increase in the probability of negative jumps than in the probability of positive jumps. In other words, investors view hikes in volatility as more connected to price crashes than surges. The λ_- and λ_+ estimates indicate that investors assign heavier tails to negative jumps than to positive jumps, with negative jump returns averaging -3.85% and positive jump returns averaging 2.73% .

The dynamics of the tail factor are determined by mean-reversal and jumps. The mean-reversal dictates that U_t is slowly decaying towards zero, but jumps in the tail factor, which are always positive, more than offset the decreases. Changes in the tail factor, be them slow decreases through mean-reversal or hikes via x or y jumps, affect the dynamics of the model by changing the probability of negative jumps. To interpret these changes, it is necessary to differentiate between the two types of jumps that the tail factor can be affected by. This is necessary because jumps in U_t increase the probability of future negative jumps, but its immediate and subsequent effects depend on whether U_t co-jumped with prices or jumped independently.

If U_t jumped independently, then there is an increase in the negative jump intensity,

but the current values of the market index and volatility factors are not affected. However, their future dynamics are. Indeed, an increased probability of negative jumps makes it more likely that future prices will crash and that future volatility will soar. These effects are directly reflected in the price dynamics through the compensated jump measure $\tilde{\mu}^Q$ and in the short-term volatility dynamics via the jump measure μ . Investors now assign a higher probability of crashes to the index, a higher probability of jumps to the volatility, and a higher probability of jumps to the tail factor.

If the jump in U_t was due to a price co-jump, then, in addition to a decrease in the index price, we also see an increase in the volatility due to the leverage effect. The increase in both factors translates to a higher increase in the probability of negative jumps than when U_t jumps independently. Investors now assign even higher probabilities of future crashes in the index, and hikes in the volatility and the negative jump intensity. Additionally, the index is at a lower level than before and is more volatile.

The distinguishing feature between x and y jumps is the jump in the short-term volatility factor, which boosts the increase in the jump intensity. It turns out this difference is key in understanding how the tail factor is related to the model free implied moments of returns. This connection is discussed in the next section.

4 Using the AFT Model to Interpret the Model Free Implied Moments

The 3-factor AFT model displays two sources of jumps: x jumps, which are price jumps that cause both the volatility and tail factors to jump, and y jumps, which are independent jumps in the tail factor. It is important to notice that these jumps fundamentally originate from an external change in the economy. For example, an announcement that leads to uncertainty regarding a country's trade policy could result in investors' having different opinions regarding the valuation of several companies, leading to a jump of type x .

In the AFT model, the distinguishing feature between x jumps and y jumps is the jump in the short-term volatility factor. Jumps in U_t are caused by x and y jumps, while jumps in $V_{1,t}$ can only happen due to x jumps. In both cases the probability of negative jumps increases, but it increases more when an x jump occurs. This is key in understanding how the tail factor is related to the implied moments of returns.

Jump Type	Effect
x jump	X_t , $V_{1,t}$ and U_t jump
y jump	U_t jumps

Table 2: Summary of types of jumps in the AFT model.

The implied moments are measures of the 2nd, 3rd and 4th moments of returns. Under a jump-diffusion process for the returns, IM2 approximates the expectation of the integrated volatility (diffusive volatility plus squared jumps) over the next 30 days, while IM3 and IM4 approximate the sum of jumps to the 3rd and 4th powers over the next 30 days. Thus, it is intuitive to associate changes in IM3 and IM4 to changes that are exclusively related to jumps, and changes in IM2 to changes that are related to both jumps and variance.

This intuition connects the implied moments to the AFT model. If U_t jumps independently of the market index (y jump), then there is an increase in the probability of

future negative price jumps. This increased probability is expected to reflect on IM3 and IM4, since they are related to future jump returns, and we should observe an increase in both implied moments. What about IM2? When there is a y jump, the short-term volatility factor does not jump. Nevertheless, the probability of a future volatility jump does increase, which should lead to a small increase in IM2. IM2 is also affected by the increase in expectation of future jumps. But its effect is small compared to the size of the integrated volatility. This means that the percentage change in IM2 is should be smaller than that of IM3 and IM4.

Now, if the jump in U_t is caused by a price co-jump (x jump), then the volatility factor also jumps. Therefore, not only the expectation of the sum of jump returns increase, but also the expectation of the diffusive volatility. In this case, the proportional change in IM2 is should be comparable to that of IM3 and IM4.

This intuition is based on the jump-diffusion approximations of the implied moments. But to truly connect the implied moments to the 3-factors model, it is necessary to analyze the changes in IM2, IM3 and IM4 under the returns dynamics of the AFT model. However, it is not possible to derive a closed-form solution for the implied moments in terms of the 3-factors of the model, so we rely on numerical experiments.

The AFT model is in the affine class defined by Duffie, Filipović, and Schachermayer (2003), which allows for the numerical solution of options prices without requiring to simulate the model repeatedly. To compute the options prices, I use the software by Fusari (2017). I obtain a cross-section of OTM options prices from the AFT model, for different strikes, and for a fixed tenor of 30 days. I then shock the U_t factor in two possible ways: via a price co-jump (x jump), and via an independent jump in the tail factor (y jump). After that, I obtain a new cross-section of OTM options prices. Next, I use both cross-sections to compute the percentage changes in IM2, IM3 and IM4 before and after the jumps, for different shock sizes. Table 3 summarizes the results.

Jump Type	Percentage change in					
	X_t	U_t	$V_{1,t}$	IM2	IM3	IM4
x jump (price co-jump)	2.86	0.29	1	0.25	0.21	0.24
	6.41	1.46	5	1.23	1.04	1.20
	9.06	2.92	10	2.45	2.07	2.40
	12.82	5.85	20	4.91	4.15	4.83
y jump (independent jump)			1	0.11	0.19	0.20
			5	0.56	0.97	1.02
			10	1.13	1.94	2.03
			20	2.25	3.88	4.07

Table 3: Results of the numerical experiment using the AFT model to compute changes in the implied moments due to x and y jumps. Parameters used in the experiment are the same as estimates from Andersen, Fusari, and Todorov (2015b). The base level of U_t is 4, and the base level of the volatility factors is given by their long-run values.

The first rows show the percentage changes in the risk-neutral implied moments when there is an x jump, causing the volatility and tail factor to co-jump. For comparison reasons, I fix the jump sizes in $V_{1,t}$ to be 1%, 5%, 10% and 20%, and then back-out the required jump sizes in the index price to generate such moves in the volatility factor. In this case, the change in IM2 is close to that of IM3 and IM4, and the same is observed for different jump sizes.

The last rows of the table show percentage changes in the risk-neutral implied moments when the tail factor jumps independently of the market index. As U_t jumps, all implied moments increase, but IM3 and IM4 increase proportionally more than IM2. This is true for different jump sizes, as well as different base levels for the tail factor (see the Appendix for more tables).

The numerical experiments results indicate that the intuition connecting the implied moments to the factors in the AFT model is correct. Thus, under the assumptions of the AFT model, we can interpret the implied moments in terms of price co-jumps and independent tail factor jumps. If the tail factor is indeed a feature of the risk-neutral world, there should be evidence for its existence based on the model free implied moments computed from options data. More specifically, if we compute the implied moments in high frequency, we can use the techniques from high-frequency econometrics to identify big moves in the implied moments, and verify whether they follow the dynamics of the AFT model. For example, if there is a jump in the market index, then we should observe big moves in IM2, IM3 and IM4. If there is an independent jump in the tail factor, then the change in IM2 should be small compared to the change in IM3 and IM4. Using high-frequency data on the implied moments and a co-jump test between the series and the market index, it is possible to assess whether the implied moments do move as implied by the AFT model. Furthermore, because there are only positive jumps in U_t and $V_{1,t}$, the same should be true for the implied moments: big moves in IM2, IM3 and IM4 should always be positive. Lastly, we should also observe more moves of similar size between IM3 and IM4, than between IM2, IM3 and IM4.

The analysis of model free implied moments based on the AFT model is a first step in understanding what affects market's view of future risk. In the next section we analyze whether the implications of the AFT model hold in the implied moments.

5 Analyzing the Implied Moments based on the AFT Model Implications

Section 4 discussed the interpretation of the implied moments in terms of jumps in the tail factor of the AFT model. The numerical experiments suggested that jumps in the tail factor increase the expectation of future negative jumps in the market index, leading to increases in the implied moments. The experiments also suggested that the implied moments increased differently depending on the source of the jump in the tail factor. If the jump was a y jump, the percentage change of IM3 and IM4 would be larger than that of IM2. But if it was an x jump, then all implied moments would have approximately the same percentage changes. In this section, we analyze these implications using the model free measures.

5.1 Jump Returns in the Market Index and in the Implied Moments

To analyze the connection between the implied moments and the AFT model, we first look at the number and size of jump returns on the market index and on the implied moments, summarized on Table 4.

The SPY column in the table shows the average values of diffusive and jump returns for the market index. The jumps in the market index are jumps under the physical

Description (averages over 2007-2016 in %)		SPY	IM2	IM3	IM4
Positive	Continuous Returns	0.06	0.64	1.02	1.42
	Jump Returns	0.28	6.52	13.49	23.76
	Number of Jumps	151	459	1764	2099
Negative	Continuous Returns	-0.06	-0.62	-0.93	-1.29
	Jump Returns	-0.29	-5.49	-12.50	-22.05
	Number of Jumps	137	444	1544	1731

Table 4: Average continuous and jump returns of SPY, IM2, IM3 and IM4 over 2007-2016. The jump returns in SPY and the big returns in the implied moments were obtained via jump separation with a threshold parameter $\alpha = 4$.

measure. There about as many positive jumps as there are negative jumps, and both have similar magnitudes. The same holds true if the analysis is broken down year by year (refer to Table 16 in the Appendix).

The jumps in the implied moments are jumps generated under the risk-neutral measure. For IM2 there is a similar number of positive and negative jumps, but the positive jump returns have a higher magnitude than the negative jumps, on average. The jump returns in IM2 are substantially larger than those in the market index, with an average difference of more than 5 percentage points. Additionally, the number of jumps in IM2 is three times bigger the number of jumps in the market index.

Under the AFT model, negative jumps in the market index cause both the volatility and the tail factor to co-jump, in turn leading to a positive jump in IM2. The difference between the number of positive jumps in IM2 and the number of negative jumps in SPY is supportive of independent jumps in the tail factor (y jumps). If we consider the 137 negative jumps in SPY to coincide with 137 of the positive jumps in IM2 (this will be formally tested), then there are 322 positive jumps in IM2 that are potentially due to y jumps. Indeed, it was argued that y jumps lead to changes in all of the implied moments. Thus, for big enough y jumps, it is possible that the changes in IM2 would be classified as jumps, explaining the 322 big positive returns in IM2.

The column for IM3 shows that its jumps are bigger than the jumps in IM2, with an average difference of about 6 percentage points. It also shows that IM3 jumps more than three times as often as IM2, and eleven times as often as the market index. Comparing the number of jumps in IM3 to the number of jumps in the market index, it is clear that price co-jumps alone are not enough to explain the dynamics of the implied moments. Again, y jumps in the tail factor could help explain the difference. Indeed, if y jumps in the tail factor are prevalent, then we would identify more jumps in IM3 than in the market index, and the average IM3 jump return would be higher than that of IM2.

The column for IM4 shows that it has a slightly higher number of positive jumps than negative jumps, and a small difference in the magnitude of the jump returns. In addition, the number of jumps in IM4 is comparable to the number of jumps in IM3, but their magnitudes are different. The numerical experiments under the AFT model indicated that jumps in the volatility and in the tail factor should cause IM3 and IM4 to move in increasing proportions, which is what we observe in the data. The data shows that the average jump returns in IM3 are smaller than the average jump returns in IM4.

Overall, there is evidence that all implied moments have various jump returns, some of which can be explained by price co-jumps, but others that are not as straightforward. These other jumps could be explained by the tail factor in the AFT model. The explana-

tion relies on how jumps in the tail factor change the probability of future jump returns, and leads to simultaneous jumps in all of the implied moments. To assert the plausibility of this explanation, we analyze how coincidental are the jumps in the market index and in the implied moments.

5.2 Co-Jumps between the Market Index and the Implied Moments

In order to assess whether the market index and the implied moments co-jump, we implement the co-jump tests proposed by Jacod and Todorov (2009). To do so, for each of the three pairs of market index and implied moment (SPY and IM2, SPY and IM3, and SPY and IM4), we partition the sample of 2448 days into four different types of days: A, B, C and D. Each type is characterized by whether the market index and one of the implied moments jumped in the same day. Days of type A are those in which the market index and the implied moment did not jump. That is, at any given day of type A, no jump was identified in either series. Days of type B are those in which the implied moment jumped, but the market index did not. Under the AFT model, the jumps in these days are explained by jumps in the tail factor. Days of type C are the opposite: the implied moment did not jump, but the market index did. There is an important caveat to notice on days of type C. Whenever the market index jumps, so must the options prices, and, by extension, also the implied moments. However, the jumps in the implied moments could be small, since they are a non-linear combination of the options prices, and if so, they will not trigger the threshold that separates jumps from diffusive moves. Therefore, the days of type C are those in which the price co-jump is small so that the jumps in the implied moments cannot be separated from their diffusive moves. Days of type D are those in which both the implied moment and the market index jump. Under the AFT model, the jumps in these days are explained by price co-jumps, which leads to large jumps in the negative jump intensity, and in all the implied moments. Table 5 below summarizes the partitions for each of the pairs.

Type of Day	Description	IM2	IM3	IM4
A	Neither Jumped	1661	665	480
B	IM Jumped, SPY did not	535	1531	1716
C	SPY Jumped, IM did not	79	51	45
D	Both Jumped	173	201	207
Total Days in Sample		2448		

Table 5: Partition of days according to whether the market index and one of the implied moments jumped on the same day. Each column represents a partition of the days in the sample based on the pair of the market index and one of the implied moments, for a total of three different partitions.

If we sum rows B and D, we recover the number of days in which each implied moment jumped. This number is different from the total number of jumps, because there are days with more than one jump. Summing rows C and D gives the number of days in which the market index jumped.

Observe that there is a positive number of days of type C, and that there are more days of type C for IM2. This finding is possibly consistent with the existence of a tail factor. Small price co-jumps and small independent jumps in the tail factor could lead

to small moves in the implied moments, which are hard to separate from diffusive moves, thus leading to days of type C. And, as argued previously, identifying jumps in IM2 is harder than in IM3 and IM4, so it is natural to have a higher number of type C days for IM2 than for IM3 and IM4.

One of the implications of the AFT model is that x jumps should cause all implied moments to move. Since x jumps are jumps in the market index, the number of days in which all of the series jump (D days) should be the same. The values in row D seem to be consistent with this implication. Indeed, there is a similar number of days in which the market index and the implied moments jump. The small difference between the number of D days for IM2 and IM3 can be attributed to small jumps in the market index. While this indicates that jumps in the market index and in the implied moments happen in the same day, it does not offer evidence on whether they happen at the same time. To test for that, we use the days of type D to run the Jacod-Todorov co-jump test between the market index and each of the implied moments. The null hypothesis of this test is that there is at least one common jump between two series in a given day. Rejecting the null hypothesis, thus, is interpreted as evidence that the two series do not have common jumps at a given day. For each of the type D days, we test the null hypothesis at a significance level of 1%. Table 6 summarizes the results.

Co-jump tests between SPY and one of the IM measures on D-type days	IM2	IM3	IM4
No evidence for co-jumps	62	148	169
Evidence for co-jumps	111	53	38

Table 6: Summary of the co-jump tests for days in which the market index and the implied moments jumped. Follows Jacod and Todorov (2009), and uses a significance level of 1%. The null-hypothesis is that there is at least one common jump between both series in the tested day.

The last row in the table shows that in 111 days there is at least one co-jump between the market index and IM2. This is evidence that price jumps do lead to changes in the risk-neutral expectation of the future diffusive volatility and jumps, IM2. Now, the co-jump tests for IM3 and IM4 reveal that both have a similar number of co-jumps with the market index, but less so than IM2. Nonetheless, there is evidence that for about 25% of the D-type days, price jumps lead to jumps in the risk-neutral expectation of future jump returns.

There are two immediate explanations for the difference in the number of co-jumps between the implied moments and the market index. First, it could be that the effect of x jumps in the jump intensity is not as strong as suggested by the estimates of the AFT model. In fact, according to Andersen, Fusari, and Todorov (2015b), the estimated impact of price jumps in the tail factor (captured by ρ_u) is not well identified, so its estimate of 0.5 could be misleading. For example, a weaker impact of x jumps in the jump intensity would lead to a smaller number of identifiable jumps in IM3 and IM4, than in IM2. Second, it is conceivable that the implied moments jump a few minutes after the jump in the market index, a case that is not part of the Jacod-Todorov co-jump test. To investigate if the second explanation is plausible, we compute the average distance (in minutes) between the jumps in the implied moments and the jumps in the market index. Table 7 summarizes the results.

The first row of numbers shows that jumps in the market index coincide the most with jumps in IM2. From the jumps in IM2 that are not coincidental, 29 occur after a

		IM measures		
		IM2	IM3	IM4
Time difference between jumps in SPY and in one of the IM measures that happen on the same day	Number of occurrences	143	59	39
SPY and IM jumps coincide	Number of occurrences	29	92	106
	Number of IM jumps within 10 min.	5	11	16
	Number of IM jumps within 30 min.	16	29	33
	Time difference between jumps (median, in minutes)	25	75	60
SPY jumps before jump in IM	Number of occurrences	14	51	61
	Number of IM jumps within 10 min.	2	13	13
	Number of IM jumps within 30 min.	6	24	23
	Time difference between jumps (median, in minutes)	52	45	50
IM jumps before jump in SPY	Number of occurrences	14	51	61
	Number of SPY jumps within 10 min.	2	13	13
	Number of SPY jumps within 30 min.	6	24	23
	Time difference between jumps (median, in minutes)	52	45	50

Table 7: Timing between jumps in SPY and in one of the IM measures.

jump in SPY, with 5 of the lagged jumps occurring within 10 minutes, and 16 within 30 minutes. It is possible to associate these lagged jumps to changes in the market index, and interpret the time difference as how long investors take to update their beliefs about future variance (and update the options prices to reflect that). In this sense, the table presents evidence that 55% of the lagged jumps in IM2 could be related to jumps in SPY.

The first row of numbers in the table also shows that most of the market index jumps do not coincide with jumps in IM3 and IM4. From the jumps in IM3 and IM4 that are not coincidental, most occur after a jump in SPY, with approximately 30% of the lagged jumps occurring within 30 minutes. The remaining lagged jumps take more than an hour to occur, and are unlikely to be related to the jump in SPY. Therefore, the evidence for co-jumps between SPY and IM3 and IM4 is mixed. The Jacod-Todorov tests reveal that there are some co-jumps, but the timing difference for the lagged jumps confirms that most of them are unlikely to be related to jumps in the market index. This implies that jumps in IM3 and IM4 are less related to jumps in SPY. Under the AFT model, this can be achieved by having a smaller value for ρ_u .

The last four rows of the table analyze whether it is plausible for changes in the risk-neutral world (investors beliefs) to lead to changes in the physical world (jump in the market index). Notice that there is a substantial number of jumps in the market index that are preceded by jumps in the implied moments. For IM2, there are 14 preceding jumps, while for IM3 and IM4 this figure is around four times higher. About 40% of the preceding jumps coming from IM2, IM3 and IM4 occur within 30 minutes before jumps in the market index. These numbers indicate that some jumps in the implied moments could be related to changes in the physical world.

Another implication of the AFT model is that IM3 should always co-jump with IM4. Any jump in the tail factor affects the probability of future jumps, which directly impact IM3 and IM4. Going back to Table 5, rows B and D show two things about IM3 and IM4. First, on most of the days where there are no market index jumps, there are jumps in IM3 and in IM4. Under the AFT model, this can only happen if there are many more y jumps in the tail factor than x jumps. Second, on the days where there are market index jumps, the number of jumps in IM3 and IM4 is about the same. This is expected under the AFT model, since x jumps should cause all implied moments to move. Therefore, there is evidence in favor of the tail factor explanation for co-jumps between IM3 and IM4. Like before, to actually test whether IM3 and IM4 do co-jump, we run Jacod-Todorov co-jump tests between the implied moments, two at a time. Table 8 summarizes the results.

The column named "IM3 and IM4" shows the test results for co-jumps between IM3 and IM4 on two different types of days: when SPY jumped, and when SPY did not

Co-jump tests between two of the IM measures		IM3 and IM4	IM2 and IM3	IM2 and IM4
On days where SPY jumped	no evidence for co-jumps	50	93	113
	evidence for co-jumps	151	80	60
On days where SPY did not jump	no evidence for co-jumps	356	234	278
	evidence for co-jumps	1175	301	257

Table 8: Jacod-Todorov co-jump tests between two of the implied moments at a time. The null hypothesis is that there is at least one common jump between the two series on a given day. The test is repeated for multiple days, and rejection of the null is based on a significance level of 1%.

jump. We expected to find evidence that on most of the days there is at least one co-jump between the two series. Indeed, it is what the co-jump tests indicate: both on days when SPY jumps and when it does not, more than 75% of the tests indicate that there is at least one co-jump between IM3 and IM4. This is evidence in favor of the tail factor explanation.

The remaining columns of the table are used to check another implication of the AFT model: IM2 should co-jump with IM3 and IM4 when SPY jumps, but have fewer identifiable jumps when SPY does not jump. The results show that when SPY does jump, there are few co-jumps between IM2 and the other implied moments. This was expected, since we saw that IM3 and IM4 are less affected by jumps in the market index than IM2. Now, when SPY does not jump, there is evidence of co-jumps between IM2 and the other implied moments for about half of the days. This fits the explanation that y jumps lead to higher percentage changes in IM3 and IM4 than in IM2.

5.3 Weaknesses of the AFT Model

The AFT model provides a helpful guidance to interpret the data, and it allows for the interpretation of the risk-neutral moments in terms of its factors. However, the analysis of the implied moments and how it relates to jumps in the market index have identified some weaknesses in the model. These weaknesses are now discussed.

Table 4 displayed the number and size of jump returns on the market index and on the implied moments. It shows that there are negative jumps in IM2, which should not happen under the AFT model dynamics. Negative jumps in IM2 could be explained by either negative jumps in the volatility factor or in the tail factor. These negative jumps were not included in the AFT model due to identification issues, but could be relevant to explain the data. For this reason, the formal tests for co-jumps previously discussed include both negative and positive jumps.

The table also displayed the average jump return for the IM3 and IM4. The numerical experiments from Section 4 indicated that we should observe bigger jumps in IM4 than in IM3. This is what we observe in the data, but in a much larger magnitude than what was indicated by the experiments. Indeed, the experiments indicated a difference of no more than 1 percentage point, but the difference in average jump returns between IM3 and IM4 is of about 9 percentage points. This indicates that estimating the model dynamics at higher-frequency might be necessary to better understand the changes in the risk-neutral moments.

The co-jump tests also motivate the estimation of the model with high-frequency data. Table 6 indicated that there are fewer than expected co-jumps between the market index and IM3. And Table 7 showed that an explanation based on time delays between

jumps was not likely to account for all of the mismatched jumps. This indicates that a plausible explanation for the number of co-jumps is based on the effect of x jumps on the tail factor, captured by the ρ_u parameter. This parameter was estimated with high standard errors in Andersen, Fusari, and Todorov (2015b), but the high-frequency data indicates that a smaller value could be more plausible.

These weaknesses provide guidance for improving future models, and the lack of stronger faults suggest that the dynamics of the AFT model are reasonable to describe the options market.

6 Time Series Properties and Predictability of the Implied Moments

The implied moments are model free measures of the risk-neutral expectations of moments of returns. It is possible to use all of the implied moments to recover the implied skewness and kurtosis of market returns. Compared to IM3 and IM4, the implied skewness and kurtosis are more straightforward to interpret, motivating their use in what follows.

Since the implied series of variance, skewness and kurtosis were computed at the high-frequency and are model free, it is possible to study their time series properties directly. In the next section we apply the analysis of Andersen, Bollerslev, et al. (2001) to the model free measures of variance, skewness and kurtosis.

6.1 Time Series Properties of Implied Variance, Skewness and Kurtosis

The implied moments are risk-neutral expectations over the next 30-days. Characterizing the unconditional distribution of these implied measures provides valuable information about the market's view regarding the return process and has implications to risk management, portfolio allocation and asset pricing.

Table 9 below shows the summary statistics of the implied variance, skewness and kurtosis. It also displays the summary statistics for transformations of the implied variance and kurtosis. Notice that in Andersen, Bollerslev, et al. (2001) the authors can recover their volatility measure on a daily basis by using intra-day data. However, in the case of the implied moments we are able to recover their values still in high-frequency by using intra-day data.

	Implied Variance	Implied Skewness	Implied Kurtosis	$\log \sqrt{\text{Implied Variance}}$	$\log \text{Implied Kurtosis}$
Mean	4.74E-03	-2.51	18.29	-2.88	2.76
Variance	4.59E-05	0.54	114.47	0.15	0.29
Skewness	5.00	-0.74	2.01	1.11	-0.21
Kurtosis	33.79	4.19	9.49	4.40	4.98

Table 9: Summary statistics for implied variance, skewness and kurtosis.

The distribution of the implied variance is positively skewed and has heavy tails. Its average value can be annualized to an average standard deviation of about 24% per year. The distribution of the implied skewness is closer to a normal, but is slightly negatively skewed and also has heavier tails. The implied kurtosis has a high variance and also heavy tails. The summary statistics reveal that modeling the implied moments by means

of a normal distribution would lead to a poor approximation. This is made evident in the kernel density estimates presented in Figure 5 below.

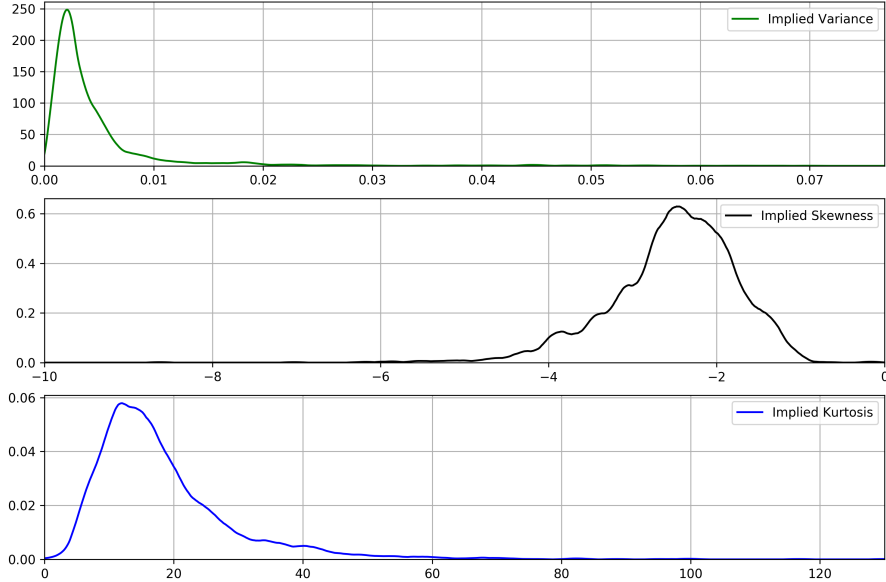


Figure 5: Kernel density estimates of unconditional distributions of the 30-days implied variance, skewness and kurtosis.

The last two columns of Table 9 display summary statistics for transformations of the implied variance and kurtosis. We use the square-root in the case of the variance in order to obtain numbers on the same scale as returns. In the case of the transformed variance the skewness and kurtosis are greatly reduced, but are still not compatible with a normal distribution. In the case of the log-kurtosis we obtain an almost symmetrical distribution, but still with heavier tails than a normal. These findings contrast with Andersen, Bollerslev, et al. (2001), where transforming the realized variance would result in an unconditional distribution close to a normal distribution. The density estimates for the transformed moments are available in the Appendix.

Next, we analyze the correlations between the implied measures. While we know that IM2, IM3 and IM4 must be highly correlated, since these are moments from the same distribution, it is not clear what the results will be after taking into account the variance (implied skewness and kurtosis). Table 10 displays the correlation between the implied variance, skewness and kurtosis.

	Implied Variance	Implied Skewness	Implied Kurtosis	$\log \sqrt{\text{Implied Variance}}$	$\log \text{Implied Kurtosis}$
Implied Variance	1	0.08	-0.14	0.82	-0.19
Implied Skewness		1	-0.94	0.23	-0.94
Implied Kurtosis			1	-0.25	0.92
$\log \sqrt{\text{Implied Variance}}$				1	-0.33

Table 10: Covariance matrix for implied variance, skewness and kurtosis.

Interestingly, the correlation between the implied variance and both the implied skewness and kurtosis is small, indicating that it is possible to have moves in the variance that

do not directly correspond to moves in skewness or kurtosis. This is still the case when we consider the transformed variance and kurtosis. The correlation between skewness and kurtosis is highly negative, indicating a tight relation between the market's expectation of skewness and kurtosis. As the implied skewness decreases, implying in more negative returns, we also get an increase in the implied kurtosis, i.e., higher probability of very negative returns.

To summarize, there is considerable variation in all of the implied measures, with a strong negative correlation between implied skewness and kurtosis. Next, we analyze the dynamics and time dependence of the implied measures, which characterize their conditional distribution. The conditional distribution of these implied measures is important in determining the fair value of financial derivatives, since the distribution of market returns is linked to the implied moments. Improving the forecast of implied variance, skewness and kurtosis has the potential to improve our understanding of the prices of financial derivatives. The conditional dependence in volatility allows for its forecast, as discussed in Andersen, Bollerslev, et al. (2001). Are similar dependencies also present in the implied measures?

To facilitate the analysis of the conditional dependency of the implied measures, we consider a coarse sample of the data, using only daily values of the implied variance, skewness and kurtosis. Figure 6 displays the time series of such values at the daily frequency (close values).

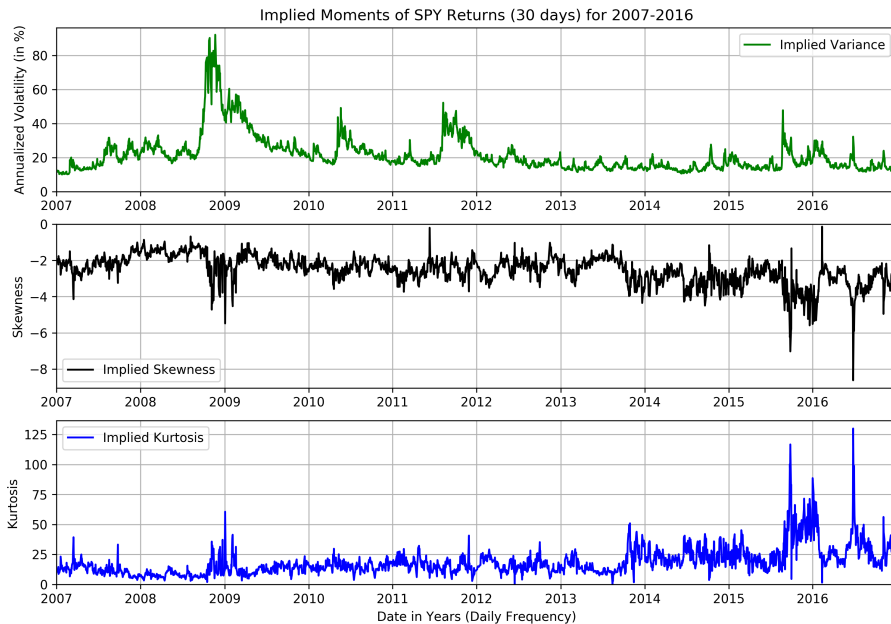


Figure 6: Time series of the implied variance, skewness and kurtosis. Daily close values.

The figure shows a high degree of variation in all of the implied measures and also strong persistence. The persistence in the implied variance is due to known volatility clustering effects. The strong dependence is confirmed by the results from the Ljung-Box test presented in Table 11 below.

All test statistics are highly significant. The persistence is also supported by the correlograms of the implied measures, shown in Figure 7.

Lags Tested	Critical Value at 99.9%	Ljung-Box Test Statistic for		
		Implied Variance	Implied Skewness	Implied Kurtosis
20	45.3	36766	21976	20665
100	149.4	70198	49724	46869

Table 11: Ljung-Box test for series of daily implied variance, skewness and kurtosis.

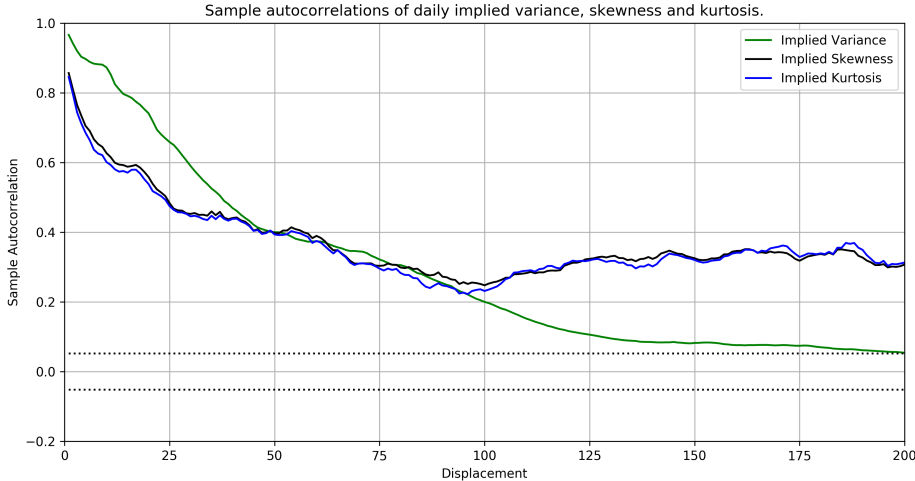


Figure 7: Correlogram of daily implied variance, skewness and kurtosis.

The correlogram shows the persistence of all implied measures. The autocorrelation of the implied variance starts at about 0.96 and decays very slowly, reaching the value of 0.19 at displacement 100 and about 0.05 at displacement 200. The autocorrelation of the implied skewness and kurtosis start at a lower value, about 0.85, but decay much slower, reaching the value of about 0.24 at displacement 100. At displacement 200, the autocorrelation of the implied skewness and kurtosis actually increases to about 0.31.

The autocorrelations decay slowly, which might indicate the presence of a unit-root. However, the augmented Dickey-Fuller test indicates that is not the case. Indeed, the null hypothesis of a unit-root is rejected at the 1% level for all implied measures. Table 12 reports the test statistics.

Critical Value at 99%	ADF Test Statistic for		
	Implied Variance	Implied Skewness	Implied Kurtosis
-3.43	-5.22	-5.93	-5.81

Table 12: Augmented Dickey-Fuller test for presence of unit-root in the implied variance, skewness and kurtosis. Reported statistics based on 27 augmentation lags.

The rejection of the unit-root null hypothesis does not rule out long memory of the non-unit-root type. To evaluate whether this is the case, we follow Andersen, Bollerslev, et al. (2001) in analyzing whether fractional integration in the daily implied measures is possible. Table 13 reports the estimates for the fractional integration parameter d .

The fractional integration parameter estimate for the implied variance is higher than 0.5, which means that the differentiated variance series is covariance stationary fractionally integrated. That is, if we consider the series of daily implied variances (IM2), then the differentiated series $(1 - L)IM2_t$ is covariance stationary if we take a fractional difference of $(1 - L)^{-0.23}$, i.e., $(1 - L)IM2_t$ is $I(-0.23)$. This result contrast with the estimates

Fractional Integration Estimate	Implied Variance	Implied Skewness	Implied Kurtosis
\hat{d}	0.67	0.46	0.46

Table 13: Fractional integration parameter estimate based on log-periodogram regression.

found by Andersen, Bollerslev, et al. (2001) for the realized variance of Dollar exchange rates. In the case of the realized variance, the authors estimated fractional differences of about 0.4 for the realized variances of exchange rates. However, the fractional integration parameter estimates for the implied skewness and kurtosis are 0.46, which is in line with the 0.4 values found in Andersen, Bollerslev, et al. (2001). In summary, the findings presented here indicate that long-memory dependency is present in all of the implied measures.

Now that we have characterized the conditional distribution of the implied variance, skewness and kurtosis, we turn to modeling these time series.

6.2 Predictability of Implied Variance, Skewness and Kurtosis

The forecast of the realized variance of stock returns has been extensively analyzed in Bollerslev, Patton, and Quaedvlieg (2016). We extend that analysis to the time series of daily implied variance, skewness and kurtosis.

Given the high dependency of the daily implied measures and the preference for parsimonious models, we consider three models for forecasting: the "No Change" model (white noise), an auto-regressive model of order 1 (AR), and the HAR model from Corsi (2009). The "No Change" model is a baseline for comparison, and its underlying assumption is that changes in each implied measure is driven by a white noise process:

$$\text{IM2}_t = \text{IM2}_{t-1} + u_t$$

Where u_t is white noise, so that the forecast of this model is given by $\mathbb{E}_{t-1}[\text{IM2}_t] = \text{IM2}_{t-1}$. Due to the high dependency of the measures, a parsimonious AR model might perform well out-of-sample. Lastly, the long-memory present in all of the implied measures motivates the use of the HAR model, which provides a parsimonious approximation to long-memory processes.

To evaluate the different models, we use a 1-step ahead quasi-out-of-sample forecast scheme. Starting with a window of 1000 observations, each model is estimated and then used to forecast the next value of each implied measure. Then, we roll the window by 1 observation and repeat the 1-step ahead forecast. This process is repeated until all observations are exhausted, and then we compute the mean squared forecast error. Table 14 reports the results.

The last column of the table above reports the mean squared (MSE) error relative to the mean squared error of the "No Change" model. The comparison of the forecast errors show that the HAR model achieves the smallest error for forecasting all of the implied measures. The forecasts from the HAR model provide a reduction in the MSE of about 6% compared to the No Change model. The reduction in MSE is more expressive for the case of forecasting the implied skewness and kurtosis, with reductions of approximately 15%. In all cases, the forecasts from the HAR model outperform the forecasts from the AR model. These results are consistent with the findings in Bollerslev, Patton, and Quaedvlieg (2016), and further contribute to the original argument by Corsi (2009) of using the HAR as an approximation to long-memory processes.

Implied Measure	Model	MSE	Relative MSE
Variance	AR	0.00000086	0.98
	HAR	0.00000082	0.94
	No Change	0.00000088	1.00
Skewness	AR	0.18002782	0.92
	HAR	0.16561120	0.85
	No Change	0.19477041	1.00
Kurtosis	AR	51.21812570	0.93
	HAR	47.68013483	0.86
	No Change	55.13580887	1.00

Table 14: Mean squared error (MSE) of 1-step ahead quasi-out-of-sample forecast for the daily series of implied variance, skewness and kurtosis. Estimation of the models is based on a rolling window of 1000 observations. Total number of observations is 2449.

7 Conclusion

The results in Section 5 show that the interpretation of the implied moments in terms of the AFT model can partially explain what we see in the data. The model implies that all the implied moments should co-jump with the market index, and that y jumps in the tail factor should lead to big moves in IM3 and IM4, and smaller moves in IM2. There is evidence that IM2 indeed co-jumps with the market index, but there is less evidence in favor of co-jumps between the market index and IM3 and IM4. This suggests that the impact of x jumps on the negative jump intensity is likely smaller than what was estimated in Andersen, Fusari, and Todorov (2015b), and motivates the estimation of the model in higher-frequency. There also is evidence in favor of y jumps. In fact, the data shows that there are more jumps in the implied moments than in the market index, and that there are more jumps in IM3 and IM4 than in IM2. However, the data also shows that there are negative jumps in IM2, which cannot happen under the AFT model. This motivates extending the model to allow for negative jumps in the volatility and tail factors.

In summary, the interpretation of the implied moments under the AFT model suggests that it is plausible for the jump intensity to change independently of the volatility. The time-varying tail factor provides explanations for jumps in the implied moments, and justifies the differences between IM2, IM3 and IM4. And, while there are discrepancies with the data, it is conceivable that a few extensions of the model would allow it to capture most of the features of the implied moments. The next section discusses suggestions in that direction.

The analysis of the time series of the implied variance, skewness and kurtosis showed that all series display long-memory. The high dependency of these implied measures were explored in forecasting, where we concluded that the HAR model provides a reduction in quasi-out-of-sample mean squared error when compared to alternative models.

8 Suggestions for Future Research

Analyzing the jumps in the implied moments in view of the implications of the AFT model indicated that a tail factor is indeed sensible. However, the previous analysis alone does not tell us why such a factor exists in the first place, and why it jumps independently. To answer these questions, I suggest the estimation of the AFT model using high-frequency

data. The estimation with high-frequency data allows for the recovery of the tail and volatility factors when there are big moves in the implied moments. Since the implied moments are model free and related to variance and jump risk, it would be possible to verify when jumps in IM3 are due to jumps in the tail factor or due to jumps in the volatility factor. Indeed, by recovering the high-frequency values of the factors it would be possible to check if most of the jumps in IM3 are related to increases in the tail factor, and if jumps in IM2 are related to increases in the volatility factor.

8.1 Estimation of the AFT Model with High-Frequency Data

In Andersen, Fusari, and Todorov (2015b), the authors estimate the model using only end-of-the-day prices, sampled every Wednesday. To answer the question of why a tail risk factor exists it would be needed to estimate the AFT model using high-frequency options data, sampled every minute. The benefits are twofold: it allows for the recovery of the state vector in high-frequency, and the estimation of the model parameters with potentially smaller standard deviations than found by Andersen, Fusari, and Todorov (2015b).

The state vector in high-frequency can be used conjointly with high-frequency econometrics theory to identify big moves in the tail and volatility factors, and compare those moves to the changes in the implied moments over time. I expect that whenever there are big moves in IM3 and IM4, but not in IM2, there will be moves in the tail factor, but not in the market index or in the volatility factor. And, at times when there are jumps in the market index, we should see jumps in the short-term volatility factor, and smaller moves in the tail factor.

The reduced standard deviations can help pin down the value of the parameters that could not be well estimated with weekly data by Andersen, Fusari, and Todorov (2015b). Most importantly, it could pin down ρ_u , which dictates the importance of price jumps to jumps in the tail factor. As discussed in Section 5, this parameter is potentially relevant to solving some of the inconsistencies between the model and the data.

To estimate the AFT model with high-frequency data, a possible strategy is to follow Andersen, Fusari, and Todorov (2015b), where the parameter estimates are obtained by minimizing a quadratic loss function. This loss function computes the difference between the observed and model implied options prices, but instead of using dollar values, it uses prices converted to Black-Scholes implied volatility (BSIV). The BSIV is a nonlinear transformation that takes options prices into volatilities implied by the Black-Scholes model. It is commonly used by investors to quote and trade options, and is a way to stabilize options prices. The loss function also contains a regularization term that prevents the model spot volatility from distancing from the market spot volatility, which is estimated using the high-frequency data on the S&P 500 index.

Denote the model parameters and the state vector by:

$$\begin{aligned}\theta &\equiv \{(\kappa_1, \bar{v}_1, \sigma_1, \mu_1, \rho_1), (\kappa_2, \bar{v}_2, \sigma_2, \mu_2, \rho_2), (\kappa_u, \mu_u, \rho_u), \\ &\quad (\lambda_-, \lambda_+), (c_0^-, c_1^-, c_2^-, c_u^-), (c_0^+, c_1^+, c_2^+, c_u^+) \} \\ Z_t &\equiv \{V_{1,t}, V_{2,t}, U_t\}\end{aligned}$$

The minimization problem of the loss function is written as:

$$\begin{aligned} \left(\{\hat{V}_{1,t}, \hat{V}_{2,t}, \hat{U}_t\}, \hat{\theta} \right) &= \underset{\{V_{1,t}, V_{2,t}, U_t\}_{t=1,\dots,T}, \theta \in \tilde{\Theta}}{\operatorname{argmin}} \sum_{t=1}^T \frac{1}{V_t^{ATM}} (\text{OptionBSIVFit}_t + \lambda \cdot \text{VolatilityFit}_t) \\ \text{OptionBSIVFit}_t &= \frac{1}{N_t} \sum_{j=1}^{N_t} [\text{BSIV}_{market}(t, K_j, \tau_j, \Theta_j(K_j, \tau_j)) - \text{BSIV}_{model}(K_j, \tau_j, Z_j, \theta)]^2 \\ \text{VolatilityFit}_t &= \left(\sqrt{\hat{V}_t^n} - \sqrt{V(Z_t, \theta)} \right)^2 \end{aligned}$$

In the VolatilityFit_t equation, \hat{V}_t^n is the spot diffusive volatility estimator based on high-frequency SPY data, and $V(Z_t, \theta) \equiv V_{1,t} + V_{2,t} + \eta^2 U_t$ is the spot diffusive volatility under the AFT model. In the OptionBSIVFit_t equation, N_t is the number of options available in the cross section at time t , and $\Theta_j(K_j, \tau_j)$ is the market price of the j th option in the cross section, which has strike price K_j and tenor τ_j .

Notice that the entire panel of options is used in the estimation. Indeed, OptionsBSIVFit_t is computed for every day of the sample ($t = 1, \dots, T$), and itself is an average of the model fit to the cross section of options on that day ($j = 1, \dots, N_t$).

Given the non linearity of the loss function and the high number of parameters, Andersen, Fusari, and Todorov (2015b) minimize the loss function using the Markov Chain Monte Carlo estimation as in Chernozhukov and Hong (2004).

8.2 Additional Extensions

Jumps in the implied moments are fundamentally due to changes in the economy, so a natural extension of this work is understanding what could be the economic reason for such jumps in the first place. In other words, what are the different causes of x and y jumps? What could lead to co-jumps in IM3 and IM4, but only small moves in IM2? It could be possible to understand what triggers changes in investors' expectations about future crashes by determining the size of the jumps in the factors (tail and volatility) and associating them with news. Indeed, by looking at news articles around jumps in the implied moments, it might be possible to extract the information related to those jumps and motivate the changes in the tail factor.

In order to extract this information, the interested researcher could follow the machine learning methods developed in Taddy et al. (2015) and Kelly, Manela, and Moreira (2018). However, there are two main challenges in this approach. First, is obtaining a news data set that covers the main economic and financial events since 2007, and in high-frequency. An ideal source would be the cover articles of important newspapers, and the news articles that are released throughout the day. Second, is the computational power for estimating such a model. Even though the model in Kelly, Manela, and Moreira (2018) can be estimated in parallel, the use of high-frequency text data is computationally demanding, and could require either a long estimation time, or the use of a cluster of computers. Now, having extracted the important parts of the text that relate to the changes in the implied moments, it would be possible to understand what are the economic fundamentals that changes the market's view of future returns, ultimately motivating changes to the way returns are modeled under the risk-neutral distribution.

Lastly, there are also two other possible extensions to this work. First is the analysis of the statistical properties of the model-free skewness and kurtosis following Andersen, Bollerslev, et al. (2001), and their use in explaining the cross-section of returns. Second is

developing an econometric framework that makes use of the model-free implied moments to test whether options pricing model can match the risk-neutral moments.

References

- Andersen, Torben G and Tim Bollerslev (2018). *Volatility*. Edward Elgar Publishing Limited. URL: <https://doi.org/10.4337/9781788110624>.
- Andersen, Torben G, Tim Bollerslev, et al. (2001). “The distribution of realized exchange rate volatility”. In: *Journal of the American statistical association* 96.453, pp. 42–55. URL: <https://doi.org/10.1198/016214501750332965>.
- Andersen, Torben G, Oleg Bondarenko, and Maria T Gonzalez-Perez (2010). “A Corridor Fix for High-Frequency VIX: Developing a Coherent Volatility Measure”. In: URL: <https://www.researchgate.net/publication/228840312>.
- (2015). “Exploring return dynamics via corridor implied volatility”. In: *The Review of Financial Studies* 28.10, pp. 2902–2945.
- Andersen, Torben G, Nicola Fusari, and Viktor Todorov (2015a). “Parametric inference and dynamic state recovery from option panels”. In: *Econometrica* 83.3, pp. 1081–1145. URL: <https://doi.org/10.3982/ECTA10719>.
- (2015b). “The risk premia embedded in index options”. In: *Journal of Financial Economics* 117.3, pp. 558–584. URL: <https://doi.org/10.1016/j.jfineco.2015.06.005>.
- Audrino, Francesco and Matthias R Fengler (2015). “Are classical option pricing models consistent with observed option second-order moments? Evidence from high-frequency data”. In: *Journal of Banking & Finance* 61, pp. 46–63. URL: <https://doi.org/10.1016/j.jbankfin.2015.08.018>.
- Bakshi, Gurdip, Charles Cao, and Zhiwu Chen (1997). “Empirical performance of alternative option pricing models”. In: *The Journal of finance* 52.5, pp. 2003–2049. URL: <https://doi.org/10.1111/j.1540-6261.1997.tb02749.x>.
- Bakshi, Gurdip, Nikunj Kapadia, and Dilip Madan (2003). “Stock return characteristics, skew laws, and the differential pricing of individual equity options”. In: *The Review of Financial Studies* 16.1, pp. 101–143. URL: <https://doi.org/10.1093/rfs/16.1.0101>.
- Bakshi, Gurdip and Dilip Madan (2000). “Spanning and derivative-security valuation”. In: *Journal of financial economics* 55.2, pp. 205–238.
- Banz, Rolf W and Merton H Miller (1978). “Prices for state-contingent claims: Some estimates and applications”. In: *Journal of Business*, pp. 653–672. URL: <https://www.jstor.org/stable/2352654>.
- Bates, David S (2000). “Post-'87 crash fears in the S&P 500 futures option market”. In: *Journal of Econometrics* 94.1-2, pp. 181–238. URL: [https://doi.org/10.1016/S0304-4076\(99\)00021-4](https://doi.org/10.1016/S0304-4076(99)00021-4).
- Birru, Justin and Stephen Figlewski (2012). “Anatomy of a Meltdown: The Risk Neutral Density for the S&P 500 in the Fall of 2008”. In: *Journal of Financial Markets* 15.2, pp. 151–180. URL: <https://doi.org/10.1016/j.finmar.2011.09.001>.
- Black, Fischer (1976). “Studies of stock price volatility changes”. In: *Proceedings of the American Statistical Association*, pp. 177–181.
- Bollerslev, Tim, Andrew J. Patton, and Rogier Quaedvlieg (2016). “Exploiting the errors: A simple approach for improved volatility forecasting”. In: *Journal of Econometrics* 192, pp. 1–18.
- Bollerslev, Tim, George Tauchen, and Hao Zhou (2009). “Expected stock returns and variance risk premia”. In: *The Review of Financial Studies* 22.11, pp. 4463–4492. URL: <https://doi.org/10.1093/rfs/hhp008>.

- Bollerslev, Tim and Viktor Todorov (2011). "Tails, fears, and risk premia". In: *The Journal of Finance* 66.6, pp. 2165–2211. URL: <https://doi.org/10.1111/j.1540-6261.2011.01695.x>.
- (2014). "Time-varying jump tails". In: *Journal of Econometrics* 183.2, pp. 168–180. URL: <https://doi.org/10.1016/j.jeconom.2014.05.007>.
- Bollerslev, Tim, Viktor Todorov, and Lai Xu (2015). "Tail risk premia and return predictability". In: *Journal of Financial Economics* 118.1, pp. 113–134. URL: <https://doi.org/10.1016/j.jfineco.2015.02.010>.
- Bondarenko, Oleg (2014). "Variance trading and market price of variance risk". In: *Journal of Econometrics* 180.1, pp. 81–97. URL: <https://doi.org/10.1016/j.jeconom.2014.02.001>.
- Breeden, Douglas T and Robert H Litzenberger (1978). "Prices of state-contingent claims implicit in option prices". In: *Journal of business*, pp. 621–651. URL: <https://www.jstor.org/stable/2352653>.
- Campbell, John Y and Ludger Hentschel (1992). "No news is good news: An asymmetric model of changing volatility in stock returns". In: *Journal of financial Economics* 31.3, pp. 281–318. URL: [https://doi.org/10.1016/0304-405X\(92\)90037-X](https://doi.org/10.1016/0304-405X(92)90037-X).
- Carr, Peter and Dilip Madan (2001). "Optimal positioning in derivative securities". In: URL: <https://doi.org/10.1080/713665549>.
- Cassese, Gianluca and Massimo Guidolin (2004). "Pricing and Informational Efficiency of the MIB30 Index Options Market. An Analysis with High-frequency Data". In: *Economic notes* 33.2, pp. 275–321. URL: <https://doi.org/10.1111/j.0391-5026.2004.00133.x>.
- Chen, Ren-Raw, Pei-lin Hsieh, and Jeffrey Huang (2018). "Crash risk and risk neutral densities". In: *Journal of Empirical Finance* 47, pp. 162–189. URL: <https://doi.org/10.1016/j.jempfin.2018.03.006>.
- Chernozhukov, Victor and Han Hong (2004). "Likelihood estimation and inference in a class of nonregular econometric models". In: *Econometrica* 72.5, pp. 1445–1480. URL: <https://doi.org/10.1111/j.1468-0262.2004.00540.x>.
- Christensen, Bent Jesper and Morten Ørregaard Nielsen (2006). "Asymptotic normality of narrow-band least squares in the stationary fractional cointegration model and volatility forecasting". In: *Journal of Econometrics* 133.1, pp. 343–371. URL: <https://doi.org/10.1016/j.jeconom.2005.03.018>.
- Christoffersen, Peter, Steven Heston, and Kris Jacobs (2009). "The shape and term structure of the index option smirk: Why multifactor stochastic volatility models work so well". In: *Management Science* 55.12, pp. 1914–1932. URL: <http://doi.org/10.1287/mnsc.1090.1065>.
- Christoffersen, Peter, Kris Jacobs, and Bo Young Chang (2013). "Forecasting with option-implied information". In: *Handbook of economic forecasting*. Vol. 2. Elsevier, pp. 581–656. URL: <https://doi.org/10.1016/B978-0-444-53683-9.00010-4>.
- Conrad, Jennifer, Robert F Dittmar, and Eric Ghysels (2013). "Ex ante skewness and expected stock returns". In: *The Journal of Finance* 68.1, pp. 85–124. URL: <https://doi.org/10.1111/j.1540-6261.2012.01795.x>.
- Corsi, Fulvio (2009). "A simple approximate long-memory model of realized volatility". In: *Journal of Financial Econometrics* 7.2, pp. 174–196. URL: <https://doi.org/10.1093/jjfinec/nbp001>.

- Du, Jian and Nikunj Kapadia (2012). "Tail and volatility indices from option prices". In: *Unpublished working paper. University of Massachusetts, Amherst*. URL: https://people.umass.edu/nkapadia/docs/Du_Kapadia_August2012.pdf.
- Duffie, Darrell (2001). *Dynamic asset pricing theory*. Princeton University Press.
- Duffie, Darrell, Damir Filipović, and Walter Schachermayer (2003). "Affine processes and applications in finance". In: *Annals of applied probability*, pp. 984–1053. URL: <https://www.jstor.org/stable/1193233>.
- Eraker, Bjørn, Michael Johannes, and Nicholas Polson (2003). "The impact of jumps in volatility and returns". In: *The Journal of Finance* 58.3, pp. 1269–1300. URL: <https://doi.org/10.1111/1540-6261.00566>.
- Fahlenbrach, Rüdiger and Patrik Sandås (2009). "Co-movements of index options and futures quotes". In: *Journal of Empirical Finance* 16.1, pp. 151–163. URL: <https://doi.org/10.1016/j.jempfin.2008.06.004>.
- Fan, Zhenzhen, Xiao Xiao, and Hao Zhou (2018). "Variance Risk Premium, Higher Order Risk Premium, and Expected Stock Returns". In: URL: <https://ssrn.com/abstract=3120260> (visited on 02/15/2018).
- Fusari, Nicola (July 26, 2017). *Matlab Option Pricing Toolbox*. Version 1.0. URL: <http://www.nicola.fusari.altervista.org/page0/page11/index.html>.
- Gao, George, Pengjie Gao, and Zhaogang Song (2018). "Do hedge funds exploit rare disaster concerns?" In: *The Review of Financial Studies* 31.7, pp. 2650–2692. URL: <https://doi.org/10.1093/rfs/hhy027>.
- Gao, George and Zhaogang Song (2013). "Rare disaster concerns everywhere". In: *Unpublished working paper*. URL: http://gsm.ucdavis.edu/sites/main/files/file-attachments/gaosong_rix_everywhere_20131118.pdf.
- Hao, Jinji (2017). "A Model-Free Tail Index and Its Return Predictability". In: URL: <https://dx.doi.org/10.2139/ssrn.2826577>.
- Jacod, Jean and Philip Protter (2012). *Discretization of Processes*. Springer-Verlag.
- Jacod, Jean and Viktor Todorov (2009). "Testing for common arrivals of jumps for discretely observed multidimensional processes". In: *The Annals of Statistics* 37.4, pp. 1792–1838.
- Jiang, George J and Yisong S Tian (2005). "The model-free implied volatility and its information content". In: *The Review of Financial Studies* 18.4, pp. 1305–1342. URL: <https://doi.org/10.1093/rfs/hhi027>.
- Kelly, Bryan, Asaf Manela, and Alan Moreira (2018). *Text Selection*. Working paper. URL: <http://apps.olin.wustl.edu/faculty/manela/kmm/textselection/textselection.pdf>.
- Kim, Sol and Changjun Lee (2014). "On the importance of the traders' rules for pricing options: Evidence from intraday data". In: *Asia-Pacific Journal of Financial Studies* 43.6, pp. 873–894. URL: <https://doi.org/10.1111/ajfs.12075>.
- Kim, Sol and Geul Lee (2011). "Effects of Macroeconomic News Announcements on Risk-neutral Distribution: Evidence from KOSPI200 Intraday Options Data". In: *Asia-Pacific Journal of Financial Studies* 40.3, pp. 403–432. URL: <https://doi.org/10.1111/j.2041-6156.2011.01044.x>.
- Kou, Steven G (2002). "A jump-diffusion model for option pricing". In: *Management science* 48.8, pp. 1086–1101. URL: <https://doi.org/10.1287/mnsc.48.8.1086.166>.
- Kozhan, Roman, Anthony Neuberger, and Paul Schneider (2013). "The skew risk premium in the equity index market". In: *The Review of Financial Studies* 26.9, pp. 2174–2203. URL: <https://doi.org/10.1093/rfs/hht039>.

- Martin, Ian (2017). "What is the Expected Return on the Market?" In: *The Quarterly Journal of Economics* 132.1, pp. 367–433. URL: <https://doi.org/10.1093/qje/qjw034>.
- Neuberger, Anthony (2012). "Realized skewness". In: *The Review of Financial Studies* 25.11, pp. 3423–3455. URL: <http://www.jstor.org/stable/41678620>.
- Poterba, James M and Lawrence H Summers (1986). "The Persistence of Volatility and Stock Market Fluctuations". In: *The American Economic Review* 76.5, pp. 1142–1151. URL: <http://www.jstor.org/stable/1816476>.
- Schneider, Paul (2015). "Generalized risk premia". In: *Journal of Financial Economics* 116.3, pp. 487–504. URL: <https://doi.org/10.1016/j.jfineco.2015.03.003>.
- Schneider, Paul and Fabio Trojani (2015). "Fear trading". In: URL: <https://ssrn.com/abstract=1994454> (visited on 06/14/2018).
- Taddy, Matt et al. (2015). "Distributed multinomial regression". In: *The Annals of Applied Statistics* 9.3, pp. 1394–1414. URL: <https://projecteuclid.org/euclid.aoas/1446488744>.
- Vergote, Olivier and Josep Maria Puigvert Gutiérrez (2012). "Interest rate expectations and uncertainty during ECB governing council days: evidence from intraday implied densities of 3-month Euribor". In: *Journal of Banking & Finance* 36.10, pp. 2804–2823. URL: <https://doi.org/10.1016/j.jbankfin.2012.06.014>.
- Verousis, Thanos and Owain Gwilym (2011). "Return reversals and the compass rose: insights from high frequency options data". In: *The European Journal of Finance* 17.9-10, pp. 883–896. URL: <https://doi.org/10.1080/1351847X.2010.538524>.
- Verousis, Thanos, Owain Gwilym, and Nikolaos Voukelatos (2016). "The Impact of a Premium-Based Tick Size on Equity Option Liquidity". In: *Journal of Futures Markets* 36.4, pp. 397–417. URL: <https://doi.org/10.1002/fut.21734>.
- Vilkov, Grigory and Yan Xiao (2013). "Option-implied information and predictability of extreme returns". In: URL: <https://dx.doi.org/10.2139/ssrn.2209654>.

9 Appendix

9.1 Replication of payoffs via portfolios of out of the money options

The replication of payoffs via cross-section of options is due to the results in Carr and Madan (2001). They first show that for any twice continuously differentiable function $f : \mathbb{R} \rightarrow \mathbb{R}$ we have:

$$f(Y) = f(X) + f'(X)(Y - X) + \int_0^X f''(v)(v - Y)^+ dv + \int_X^\infty f''(v)(Y - v)^+ dv$$

where $(x)^+ \equiv \max\{0, x\}$. This means that any smooth function can be written in terms of its first two derivatives, and two maximums. Now, take Y and X to be the future and current price of some asset, that is $Y = F_T$ and $X = F_t$. Then the representation above becomes:

$$f(F_T) = f(F_t) = f'(F_t)(F_T - F_t) + \int_0^{F_t} f''(K)(K - F_t)^+ dK + \int_{F_t}^\infty f''(K)(F_T - K)^+ dK$$

Notice that the terms inside the integrals are related to the payoff at time T of OTM options with strike price K :

$$\int_0^{F_t} f''(K) \underbrace{(K - F_t)^+}_{\text{payoff of OTM Put}} dK, \quad \int_{F_t}^\infty f''(K) \underbrace{(F_T - K)^+}_{\text{payoff of OTM Call}} dK$$

Writing the time T payoff of an OTM option as $M_T(K)$, we can simplify the equality to:

$$\begin{aligned} f(F_T) &= f(F_t) + f'(F_t)(F_T - F_t) + \int_0^\infty f''(K) M_T(K) dK \\ \implies \underbrace{f(F_T) - f(F_t) - f'(F_t)(F_T - F_t)}_{\equiv g(F_t, F_T)} &= \int_0^\infty f''(K) M_T(K) dK \end{aligned} \tag{4}$$

Lastly, taking the risk-neutral conditional expectations on both sides of the equation above gives the replication result:

$$\mathbb{E}_t^\mathbb{Q}[g(F_t, F_T)] = \int_0^\infty f''(K) \underbrace{\mathbb{E}_t^\mathbb{Q}[M_T(K)]}_{\equiv \Theta_t(K, T)} dK$$

The left side of the equation is the risk-neutral conditional expectation of some payoff g . The right side of the equation is a weighted portfolio of options. The weights are given by the second derivative of f , and all options have the same tenor ($T - t$), but differ in terms of the strike price. This equation says that we can recover the risk-neutral expectations of any smooth function g by purchasing a portfolio of options.

Next, we show how to use equation 4 to obtain the replicating portfolios for the different payoffs discussed in Section 2. In the case of Hellinger Swaps, I also discuss the algorithm used to compute the implied moments.

9.1.1 Replicating Portfolio for g_{VIX}

Consider the function: $f(x) \equiv -2\ln(x)$. It is such that:

$$f(F_T) - f(F_t) - f'(F_t)(F_T - F_t) = 2 \left(\frac{F_T - F_t}{F_t} - \ln \left(\frac{F_T}{F_t} \right) \right) =: g_{\text{VIX}}(r(t, T))$$

Thus, the weight function for the replication portfolio is:

$$w(K) = f''(K) = \frac{2}{K^2}$$

In consequence, the \mathbb{Q} expectation of the payoff function is replicated by the following portfolio:

$$\mathbb{E}_t^{\mathbb{Q}}[g_{\text{VIX}}(r(t, T))] = \int_0^\infty \frac{2}{K^2} \Theta_t(K, T) dK$$

9.1.2 Replicating Portfolio for g_{SVIX}

Consider the function $f(x) \equiv x^2$:

$$f(F_T) - f(F_t) - f'(F_t)(F_T - F_t) = (F_T - F_t)^2$$

Using the replication formula with f as is, we obtain:

$$\mathbb{E}_t^{\mathbb{Q}}[(F_T - F_t)^2] = \int_0^\infty 2\Theta_t(K, T) dK$$

Notice that the conditional expectations are with respect to \mathcal{F}_t . Thus, we can divide both sides by F_t^2 . Also, observe that $(e^{r(t, T)} - 1)^2 = \left(\frac{F_T - F_t}{F_t}\right)^2$. Then:

$$\underbrace{\mathbb{E}_t^{\mathbb{Q}} \left[\frac{(F_T - F_t)^2}{F_t^2} \right]}_{g_{\text{SVIX}}(r(t, T))} = \int_0^\infty \frac{2}{F_t^2} \Theta_t(K, T) dK$$

which gives the replicating portfolio for g_{SVIX} .

9.1.3 Replicating Portfolio for g_{KNS}

Start with the definition of g_{KNS} :

$$\begin{aligned} g_{\text{KNS}}(r) &= 6(2 + r - 2e^r + re^r) \\ &= 6(-\underbrace{2(e^r - 1 - r)}_{g_{\text{VIX}}} - r + re^r) \\ &= 6(r(e^r - 1) - g_{\text{VIX}}(r)) \\ &\quad \frac{F_T - F_t}{F_t} \ln \left(\frac{F_T}{F_t} \right) \end{aligned}$$

Now, consider $f(x) \equiv x \ln(x)$. Then:

$$\begin{aligned}
f(F_T) - f(F_t) - f'(F_t)(F_T - F_t) &= F_T \ln(F_T) - F_t \ln(F_t) - (1 + \ln(F_t))(F_T - F_t) \\
&= F_T \ln\left(\frac{F_T}{F_t}\right) - (F_T - F_t) \\
&= (F_T - F_t) \ln\left(\frac{F_T}{F_t}\right) - (F_T - F_t) + F_t \ln\left(\frac{F_T}{F_t}\right) \\
&= F_t \underbrace{\left[\left(\frac{F_T - F_t}{F_t}\right) \ln\left(\frac{F_T}{F_t}\right)\right]}_{r(e^r - 1)} - \underbrace{\left(\frac{F_T - F_t}{F_t}\right)}_{-(e^r - 1) + r} + \ln\left(\frac{F_T}{F_t}\right) \\
&= F_t [r(e^r - 1) - \underbrace{(e^r - 1 - r)}_{=\frac{1}{2}g_{VIX}(r)}] \\
\end{aligned}$$

Using the portfolio replication equation:

$$\mathbb{E}_t^{\mathbb{Q}} \left[F_t \left(r(e^r - 1) - \frac{1}{2}g_{VIX} \right) \right] = \int_0^\infty \frac{1}{K} \Theta_t(K, T) dK$$

Splitting the g_{VIX} term leads to:

$$\begin{aligned}
\int_0^\infty \frac{1}{K} \Theta_t(K, T) dK &= \mathbb{E}_t^{\mathbb{Q}} \left[F_t \left(r(e^r - 1) - g_{VIX}(r) + \frac{1}{2}g_{VIX}(r) \right) \right] \\
&= F_t \mathbb{E}_t^{\mathbb{Q}} \left[\underbrace{(r(e^r - 1) - g_{VIX}(r))}_{=\frac{1}{6}g_{KNS}(r)} \right] + \frac{F_t}{2} \underbrace{\mathbb{E}_t^{\mathbb{Q}}[g_{VIX}(r)]}_{\int_0^\infty \frac{2}{K^2} \Theta_t(K, T) dK} \\
\end{aligned}$$

Solving for $\mathbb{E}_t^{\mathbb{Q}}[g_{KNS}(r)]$ gives the replicating portfolio:

$$\mathbb{E}_t^{\mathbb{Q}}[g_{KNS}(r)] = \int_0^\infty 6 \frac{K - F_t}{K^2 F_t} \Theta_t(K, T) dK$$

9.1.4 Replicating Portfolio for Hellinger Swaps

Consider $f_q(x) \equiv \frac{x^q - 1}{q(q-1)}$ for $q \neq 1$:

$$\begin{aligned}
h_q(F_t, F_T) &\equiv f_q(F_T) - f_q(F_t) - f'_q(F_t)(F_T - F_t) \\
&= F_t^q \left(\frac{e^{qr} - 1 - q(e^r - 1)}{q(q-1)} \right)
\end{aligned}$$

Let's analyze the term inside the parenthesis. Denote it by $\tilde{h}(r)$. Then, by Taylor's theorem:

$$\begin{aligned}
\tilde{h}(r) &= \frac{1}{2}r^2 + \frac{1}{3!} \cdot \frac{q^2 - 1}{q-1} r^3 + \frac{1}{4!} \cdot \frac{q^3 - 1}{q-1} r^4 + \dots \\
&= \sum_{j \geq 2} \underbrace{\frac{q^{j-1} - 1}{(q-1)j!}}_{A(j, q)} r^j
\end{aligned}$$

So we know the payoff function h_q is related to powers of r of orders two and above, and we know the coefficients associated to each power. Because h_q has a replication portfolio and F_t^q is \mathcal{F}_t measurable, the payoff $\tilde{h}(r) \equiv \tilde{h}(F_t, F_T)$ also has a replication portfolio:

$$\mathbb{E}_t^{\mathbb{Q}}[\tilde{h}(F_t, F_T)] = \frac{1}{F_t^q} \mathbb{E}_t^{\mathbb{Q}}[h(F_t, F_T)] = \frac{1}{F_t^q} \int_0^\infty K^{q-2} \Theta_t(K, T) dK$$

Notice that we can multiply $\tilde{h}(r)$ by $A(2, q)^{-1} = 2$, so that the coefficient associated with r^2 is one.

To obtain other payoffs, note that $A(j, q)$ can be written as:

$$\begin{aligned} A(j, q) &\equiv \frac{1}{j!} \cdot \frac{q^{j-1} - 1}{q - 1} \\ &= \frac{1}{j!} \cdot \frac{(q-1)(q^{j-2} + q^{j-3} + \dots + q + 1)}{q-1} \\ &= \frac{1}{j!} (1 + q + \dots + q^{j-2}) \\ &= \frac{1}{j!} \sum_{i=0}^{j-2} q^i \quad \text{for } j = 2, 3, \dots \end{aligned}$$

This means that the highest power of q in $A(j, q)$ is $j - 2$. So, taking the derivative of $\tilde{h}(r)$ with respect to q , eliminates r^2 , since $A(2, q) = \frac{1}{2}$. Taking the 2nd derivative with respect to q eliminates r^3 (and r^2), since $A(3, q) = \frac{1}{3!}(1 + q)$. Taking the 3rd derivative with respect to q eliminates r^4 , and so on. In fact, taking the $j - 2$ derivative of $A(j, q)$ with respect to q , leaves only r^j (and higher powers of r):

$$A^{(j-2)}(j, q) \equiv \frac{\partial^{j-2} A(j, q)}{\partial q^{j-2}} = \frac{1}{j(j-1)}$$

This motivates defining new payoff functions with respect to derivatives of \tilde{h} . Define:

$$\begin{aligned} \tilde{g}_0(r) &\equiv \tilde{h}(r) &= \sum_{j \geq 2} A^{(0)}(j, q) r^j &= \frac{1}{2} r^2 + \sum_{j \geq 3} A^{(0)}(j, q) r^j \\ \tilde{g}_1(r) &\equiv \frac{\partial \tilde{h}(r)}{\partial q} &= \sum_{j \geq 3} A^{(1)}(j, q) r^j &= \frac{1}{6} r^3 + \sum_{j \geq 4} A^{(1)}(j, q) r^j \\ &\vdots \\ \tilde{g}_{n-2}(r) &\equiv \frac{\partial^{n-2} \tilde{h}(r)}{\partial q^{n-2}} &= \sum_{j \geq n} A^{(n-2)}(j, q) r^j &= \frac{1}{n(n-1)} r^n + \sum_{j \geq n+1} A^{(n-2)}(j, q) r^j \end{aligned}$$

Since we will take linear combination of these functions, it is helpful to normalize them so that the coefficient of the desired power of r is one:

$$\begin{aligned} g_{n-2}(r) &\equiv [A^{(n-2)}(n, q)]^{-1} \cdot \tilde{g}_{n-2}(r) \\ &= r^n + \sum_{j \geq n+1} n(n-1) A^{(n-2)}(j, q) r^j \end{aligned}$$

Notice that the transformations applied on $\tilde{h}(r)$ still allows g_{n-2} to have a replicating portfolio:

$$\begin{aligned}\mathbb{E}_t^{\mathbb{Q}}[g_{n-2}(r)] &= n(n-1) \frac{\partial^{n-2}}{\partial q^{n-2}} \int_0^\infty \frac{K^{q-2}}{F_t^q} \Theta_t(K, T) dK \\ &= n(n-1) \int_0^\infty \frac{K^{q-2}}{F_t^q} \left[\ln \left(\frac{K}{F_t} \right) \right]^{n-2} \Theta_t(K, T) dK\end{aligned}\quad (5)$$

Now, consider removing the influence of r^{n+1} from $g_{n-2}(r)$. Because the coefficient associated with r^{n+1} in $g_{n-1}(r)$ is one, we can remove r^{n+1} from $g_{n-2}(r)$ by taking the following linear combination:

$$\begin{aligned}g_{n-2}(r) - g_{n-1}(r) \cdot n(n-1)A^{(n-2)}(n+1, q) &= \\ = r^n + \sum_{j \geq n+2} [n(n-1)A^{(n-2)}(j, q) - n(n+1)A^{(n-1)}(j, q)] r^j\end{aligned}$$

It is useful to compute the coefficient associated with r^{n+1} in $g_{n-2}(r)$:

$$\begin{aligned}n(n-1)A^{(n-2)}(j, q) &= n(n-1) \frac{1 + (n-1)q}{n(n^2 - 1)} \\ &= \frac{1 + (n-1)q}{n+1} \\ &= \frac{1}{2} \quad \text{for } q = \frac{1}{2}\end{aligned}$$

And the replicating portfolio for the linear combination of the two portfolios is:

$$\mathbb{E}_t^{\mathbb{Q}} \left[g_{n-2}(r(t, T)) - \frac{1}{2} g_{n-1}(r(t, T)) \right] = \mathbb{E}_t^{\mathbb{Q}}[g_{n-2}(r(t, T))] - \frac{1}{2} \mathbb{E}_t^{\mathbb{Q}}[g_{n-1}(r(t, T))]$$

where the terms in the right side are computed as in equation (5).

This suggests the following algorithm for computing the implied moments:

1. Choose $n \in \{2, 3, \dots\}$;
2. Define $\text{IM}(n+1) \equiv \mathbb{E}_t^{\mathbb{Q}}[g_{n-1}(r(t, T))]$.
 $\text{IM}(n+1)$ depends only on returns of power $n+1$ and above.
3. Compute $\text{IM}(n) \equiv \mathbb{E}_t^{\mathbb{Q}}[g_{n-2}(r(t, T))] - \frac{1}{2} \cdot \text{IM}(n+1)$.
4. If $n = 2$ stop. Otherwise, let $n \leftarrow n - 1$ and go back to the 3rd step.

Note that the replicating portfolios are computed substituting $q = \frac{1}{2}$. $\text{IM}(n)$ computed from above depends only on r^n and on the returns to powers $n+2$ and above. The first three implied moments are denoted by IM2 , IM3 and IM4 .

9.2 Data cleaning and computation of the implied moments

The computation of the 30-days implied moments uses high-frequency data on the S&P 500 index options (SPX), and on the SPDR S&P 500 exchange-traded fund (SPY).

The data set on the SPX options was obtained from the Chicago Board Options Exchange (CBOE). The set contains quotes at the 1-minute interval level, from 2007 to 2016. The market hours are from 9:30 am to 4:15 pm EST, resulting in 405 quotes per day. Partial trading days are removed from the sample (23 in total), and the analysis is based on the remaining 2448 days. On 28 trading days there are missing values for the first minute or two at the market open. These missing values are filled with the first non-zero prices of the same day.

The data set on SPY was obtained from TickData⁴. The set contains the last closing price of every 1-minute interval, from 2007 to 2016, and is matched to the options data set.

Additionally, interest rate data is obtained from the Federal Reserve Bank of St. Louis (FRED)⁶. The series contains 1-month treasury constant maturity rate at a daily frequency, from 2007 to 2016.

The risk-neutral implied moments are recovered from payoffs that are replicated with portfolios of out of the money options. These portfolios are constructed using options with all possible strike prices in the positive line. In practice, however, the number of available strikes is finite, and so, the integrals defining the replicating portfolios must be discretized. Consider the example below:

$$\int_0^\infty \frac{\Theta_t(K, T)}{K^2} dK \approx \sum_{K=K_{\min}}^{K_{\max}} \frac{\Theta_t(K, T)}{K^2} \Delta K$$

The discretization of such integrals requires two choices. First, is the choice of the strike price range ($K_{\min} \leq K \leq K_{\max}$) over which the integral is discretized. And second, is the choice of the expiration dates of the options ($\tau \equiv T - t$).

These choices directly impact the implied moments. For example, although it seems natural to use all available strike prices in the data, doing so leads to many spurious jumps (bouncebacks) in the implied moments. This is due to the lack of liquidity in the options prices that are very out of the money. Andersen, Bondarenko, and Gonzalez-Perez (2015) analyze this problem in the context of CBOE's VIX index and propose a corridor-based solution. Another example is the choice of which tenors to consider in the computations. This is relevant because, while we want to recover 30-days implied moments, there are no options that always expire in exactly 30 days. These aspects and various other details are discussed next.

9.2.1 Time to maturity

The implied moments are computed fixing the time to maturity to 30 calendar days. A difficulty that follows from fixing the maturity is that options that expire in exactly 30 days are not available at all times. In fact, most of the time SPX options either expire a few days after or before 30 days. Following CBOE's VIX white paper⁷, I select two sets of options with different maturities (τ_1, τ_2) for constructing the implied moments. These options are chosen to have time to expiration more than 23 days and less than 37

⁶Source: <https://fred.stlouisfed.org/series/DGS1MO>

⁷See the VIX whitepaper.

days, with $\tau_1 < \tau_2$. Each set of options is used to construct a payoff replicating portfolio, generating two series of implied moments: one over the next τ_1 days, and one over the next τ_2 days. The linear interpolation of the two series gives the implied moment of returns over the next 30 days.

Other details, such as dealing with holidays, computing time to maturity in minutes, and differences between AM and PM settled options are as in CBOE's VIX white paper.

9.2.2 Strike prices and the corridor fix

Having fixed the maturity at 30 days, the next difficulty is the selection of the range of strike prices. While in general the replicating portfolio uses an infinite number of OTM options at different strike prices, the practical computation of this portfolio uses only a finite number of options with different strikes. A natural idea is to use all OTM options available in the data. This, however, leads to issues, since very out of the money options are rarely traded, and display erratic prices (given by mid-quotes) that often do not correspond to the real value of the options.

CBOE deals with this issue in the context of the VIX by proposing a selection rule for OTM options. First, start with the put option that is closest to the money. Check its bid price, and include it in the selection if it is non zero. Then, move to the consecutive put option with a lower strike price, and check for a non-zero bid price. Continue doing so until two consecutive zero bid prices are encountered, and, at this point, do not include any put option with a lower strike price. A similar rule is applied to OTM call options. Furthermore, this rule is applied whenever the index is computed, even at the minute level, since the number of options selected changes due to changing prices.

While the CBOE selection rule deals with misleading prices, it introduces a corridor effect: the number of selected options (strike range) changes from minute to minute. For this reason, the VIX not only reflects the market volatility, but also random shifts in the range of selected strikes. In fact, if one of the two consecutive zero bid prices suddenly becomes positive, then a potentially large number of options gets added to the selection, leading to artificial jumps in the series. See figure 8.

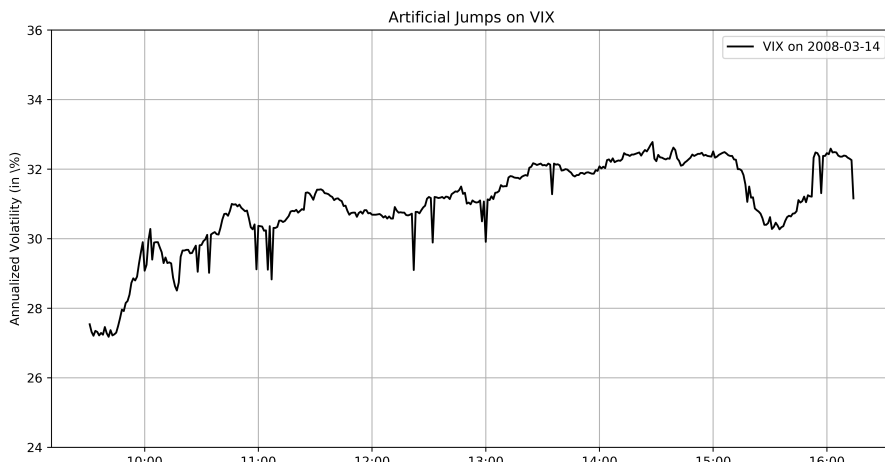


Figure 8: Multiple jumps on the VIX due to changes in the strike price corridor. Plot shows VIX (annualized volatility in percentage) over the course of a trading day in 2008.

This issue is analyzed in detail in Andersen, Bondarenko, and Gonzalez-Perez (2015). The authors propose an alternative method of selecting the options. This method is based on an endogenous ratio statistic, which is directly computed from the option prices:

$$R(K) \equiv \frac{\int_0^K (K-x)f(x)dx}{\int_0^K (K-x)f(x)dx + \int_K^\infty (x-K)f(x)dx} = \frac{P(K)}{P(K) + C(K)}$$

where K is the strike price, f is the risk-neutral density, and $P(K)$ and $C(K)$ are the prices of a put and a call with strike price K . The ratio statistic is similar to a cumulative density function, since $R(0) = 0$, $\lim_{K \rightarrow \infty} R(K) = 1$ and R is strictly increasing in K . It indicates how far in the tail a given strike price K is. If $R(K)$ is close to zero, it means K is a strike price for a very out of the money put option. If $R(K)$ is close to one, it means K is a strike price for a very out of the money call option.

The idea is to select the OTM options with strike prices that are not too much out of the money, as measured by the ratio statistic, since those have lower liquidity and their prices are more prone to microstructure noise. The range is defined by symmetric percentiles of R : $K_{\min} = R^{-1}(p) \leq K \leq K_{\max} = R^{-1}(1-p)$. Since the ratio statistic is computed from option prices, it provides a consistent way to select the strike price range. Andersen, Bondarenko, and Gonzalez-Perez (2015) further argues that the VIX index computed using the range given by the ratio statistic retains all key time-series properties of the VIX (in lower frequency), but displays less noise in higher-frequency.

Based on their results, I choose $p = 3\%$ for the truncation level with the ratio statistic, leading to higher quality mid-quotes. See figure 9 for an updated VIX computed using strike prices based on the ratio statistic. Options that fall within the range but have zero bid prices are still ignored.

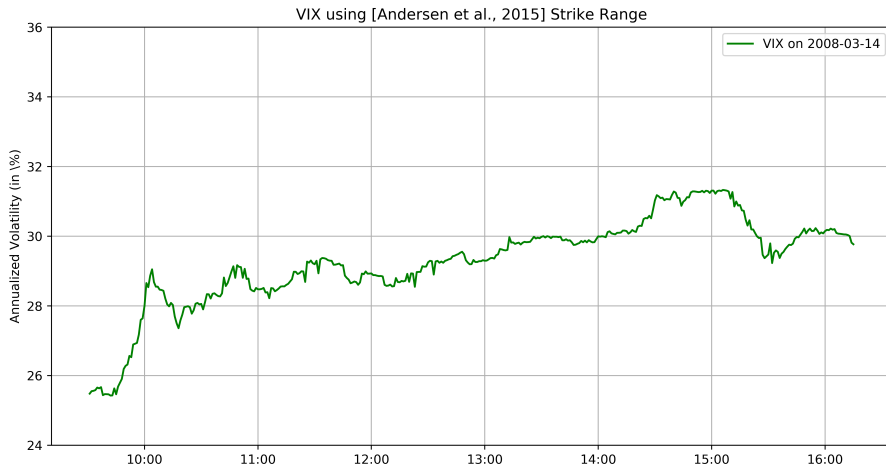


Figure 9: High-frequency VIX computed using a strike price range based on the ratio statistic from Andersen, Bondarenko, and Gonzalez-Perez, 2015. Plot shows VIX (annualized volatility in percentage) over the course of a trading day in 2008.

Notice that the jumps due to random shifts in the strike range have been smoothed over. Selecting options via the ratio statistic essentially smoothes the range of strike prices, while still allowing changes in the number of options if the tails shift.

9.2.3 Differences in liquidity of SPX options

Lastly, the composition of expiration dates of SPX options varies throughout the years, and affects the way implied moments are computed. The history of SPX options is relevant in understanding how so. SPX options were launched in 1987, and originally expired every 3rd Friday of the month. Their increasing success warranted the expansion of SPX options to include new expiration dates. In 2005, CBOE introduced SPX Weeklys, which expire on all other Fridays. However, at launch, these options had much lower liquidity than the original SPX options, but their liquidity increased substantially over the years⁸. Now, because implied moments are computed from the prices of options, it is imperative to have prices that directly reflect the real value of options. For this reason, options with low liquidity, or higher spreads, are disregarded in favor of options with high liquidity. In the case of SPX options, the liquidity is related to the expiration dates, since the original SPX options had higher liquidity than the Weeklys at launch, and for some years after that. This difference in liquidity is taken into account by the CBOE when computing the VIX index: Weeklys are only used in the computations after 2013. I follow CBOE and use SPX Weeklys only after 2013.

In summary, I follow CBOE's VIX methodology when it comes to selecting two sets of options with different tenors, the interpolation to obtain a 30 days measure, ignoring options with zero bid prices, and using Weeklys for the computations only after 2013. Having fixed the tenors, I follow Andersen, Bondarenko, and Gonzalez-Perez (2015) to select the range of strike prices to use.

9.2.4 Bounceback Filters

These cleaning procedures result in selecting cross-sections of OTM options for every minute of the day. Their prices (mid-quotes) and strikes are used to compute the implied moments of returns. One last cleaning procedure is a bounceback filter that is applied to the series of implied moments. Inspired by the bounceback filter in Andersen, Bondarenko, and Gonzalez-Perez, 2015, I use the bipower variance and jump separation threshold (see Jacod and Protter, 2012) to identify big jumps (cutoff with $\alpha = 8$). These big jumps are tracked over the next two minutes. If at least 75% of the jump is undone within one minute, or at least 80% is undone within two minutes, the jump is classified a bounceback, and its value is backfilled. In total, 171 bouncebacks were fixed.

9.2.5 No-arbitrage Filters

9.3 Additional Figures and Tables

⁸See SPX Weeklys volume chart on CBOE's website.

	IM2	IM3	IM4
Mean	0.0047	-0.0012	0.0011
Std. Deviation	0.0068	0.0042	0.0058
Minimum	0.0008	-0.0607	0.0000
Maximum	0.0653	-0.0000	0.0998
Skewness	5.0072	-8.2702	10.1778
Kurtosis	33.7543	82.1143	122.0468

Table 15: Summary statistics for the risk-neutral implied moments over the entire sample (2007-2016). These implied moments were computed at the 1 minute frequency, and averaged to 5 minutes. Values are in units over 30-days.

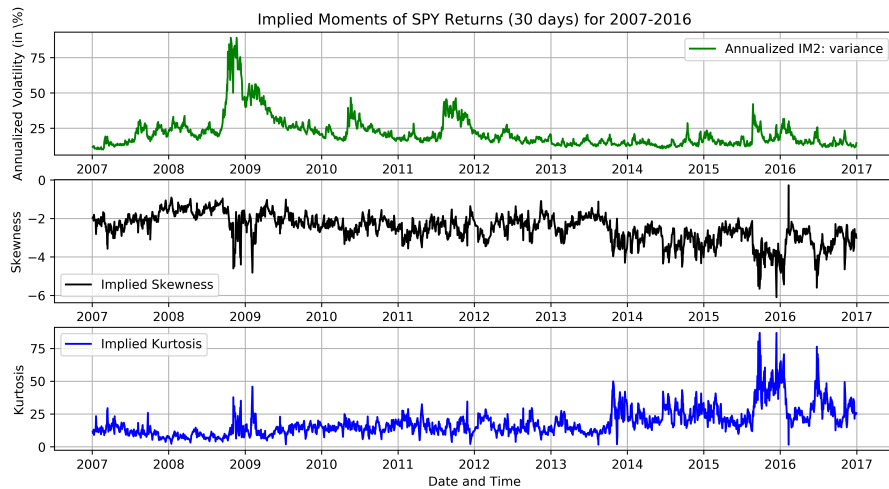


Figure 10: Time series of risk-neutral implied Variance, Skewness and Kurtosis. Values are risk-neutral expectations over the next 30 days.

Series	Description (avg. in %)	2007	2008	2009	2010	2011	2012	2013	2014	2015	2016	2007-2016
SPY	Continuous Returns	0.05	0.12	0.08	0.06	0.06	0.04	0.03	0.04	0.04	0.04	0.06
	Positive Jump Returns	0.30	0.45	0.38	0.40	0.38	0.26	0.27	0.20	0.26	0.18	0.28
	Number of Jumps	17	4	14	11	11	25	14	14	19	22	151
	Continuous Returns	-0.05	-0.12	-0.09	-0.06	-0.06	-0.04	-0.04	-0.04	-0.05	-0.04	-0.06
	Negative Jump Returns	-0.28	-0.47	-0.44	-0.42	-0.44	-0.26	-0.18	-0.16	-0.21	-0.19	-0.29
	Number of Jumps	13	8	14	19	8	17	15	18	7	18	137
	Continuous Returns	0.71	0.64	0.49	0.57	0.62	0.47	0.48	0.74	0.90	0.72	0.64
	Positive Jump Returns	11.15	12.09	5.93	4.59	4.71	4.59	2.93	4.85	6.03	3.69	6.52
	Number of Jumps	50	67	57	51	41	66	32	33	31	31	459
IM2	Continuous Returns	-0.69	-0.67	-0.47	-0.54	-0.62	-0.48	-0.46	-0.71	-0.84	-0.73	-0.62
	Negative Jump Returns	-5.41	-8.57	-6.20	-4.60	-4.14	-4.98	-3.23	-5.05	-6.11	-3.97	-5.49
	Number of Jumps	46	66	61	30	41	72	45	18	40	25	444
	Continuous Returns	0.96	1.05	0.92	0.88	0.91	0.76	0.71	1.17	1.64	1.14	1.02
	Positive Jump Returns	15.71	20.99	15.56	11.38	10.80	13.64	7.66	9.53	15.33	9.78	13.49
	Number of Jumps	193	208	196	169	159	184	146	143	204	162	1764
	Continuous Returns	-0.88	-1.08	-0.82	-0.81	-0.90	-0.72	-0.67	-1.06	-1.29	-1.12	-0.93
	Negative Jump Returns	-10.62	-17.13	-16.48	-10.36	-10.33	-13.56	-8.70	-9.93	-15.87	-8.73	-12.50
	Number of Jumps	155	184	182	143	129	167	151	108	168	157	1544
IM3	Continuous Returns	1.27	1.42	1.27	1.32	1.32	1.06	1.04	1.55	2.34	1.58	1.42
	Positive Jump Returns	24.83	30.98	29.09	19.87	18.06	26.05	14.73	16.63	33.45	17.19	23.76
	Number of Jumps	232	240	198	189	186	211	179	197	268	199	2099
	Continuous Returns	-1.18	-1.47	-1.12	-1.17	-1.29	-0.98	-0.95	-1.42	-1.84	-1.52	-1.29
	Negative Jump Returns	-18.12	-27.29	-28.18	-17.35	-16.75	-28.14	-17.44	-16.40	-31.08	-15.55	-22.05
	Number of Jumps	171	206	197	165	156	176	175	124	178	183	1731
	Avg. Number of Options	68	86	105	109	118	110	114	128	160	150	115

Table 16: Summary of jump returns in the market index and in the implied moments. Displays the average positive and negative jump returns, the number of positive and negative jumps, and the average positive and negative continuous returns. Jump returns are obtained using a threshold parameter $\alpha = 4$.

	Implied Variance	Implied Skewness	Implied Kurtosis
1-min. Frequency			
Mean	4.74E-03	-2.51	18.29
Variance	4.59E-05	0.54	114.47
Skewness	5.00	-0.74	2.01
Kurtosis	33.79	4.19	9.49
5-min. Frequency			
Mean	4.74E-03	-2.51	18.30
Variance	4.59E-05	0.54	114.85
Skewness	4.99	-0.75	2.02
Kurtosis	33.74	4.22	9.64
Daily Frequency			
Mean	4.73E-03	-2.52	18.43
Variance	4.60E-05	0.58	131.35
Skewness	4.98	-1.03	2.60
Kurtosis	33.69	6.26	15.27

Table 17: Summary statistics of implied variance, skewness and kurtosis based on different sampling frequencies. There is no substantial change in the statistics as sampling frequency decreases.

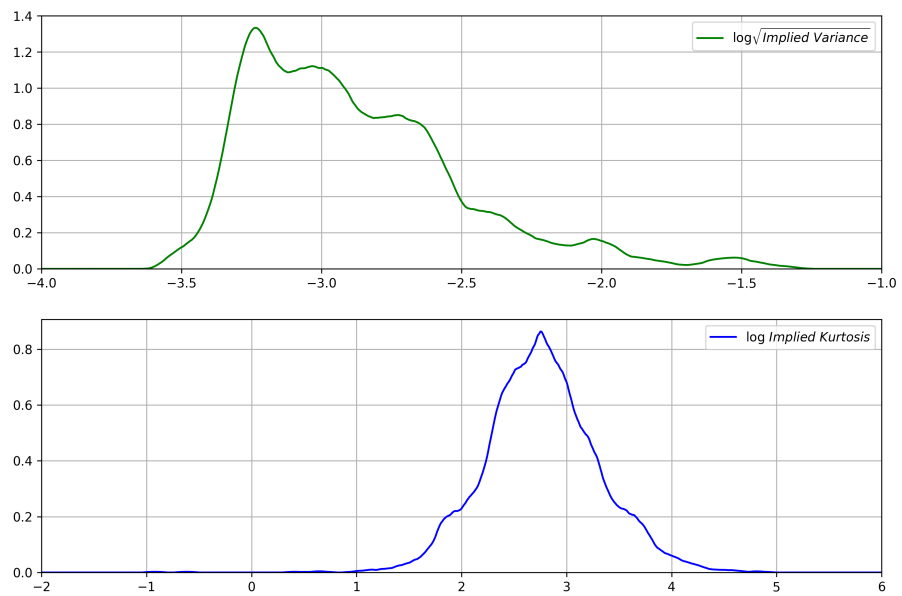


Figure 11: Kernel density estimates of non-linear transformations of the implied variance and implied kurtosis.